

UC San Diego

UC San Diego Previously Published Works

Title

Discovery of Potent Antimalarial Type II Kinase Inhibitors with Selectivity over Human Kinases.

Permalink

<https://escholarship.org/uc/item/5bd2g6s5>

Journal

Journal of medicinal and pharmaceutical chemistry, 67(2)

Authors

Wang, Lushun

Bohmer, Monica

Wang, Jinhua

et al.

Publication Date

2024-01-25

DOI

10.1021/acs.jmedchem.3c02046

Peer reviewed



Published in final edited form as:

J Med Chem. 2024 January 25; 67(2): 1460–1480. doi:10.1021/acs.jmedchem.3c02046.

Discovery of Potent Antimalarial Type II Kinase Inhibitors with Selectivity over Human Kinases

Lushun Wang[&],

Department of Chemical and Systems Biology, ChEM-H, Stanford Cancer Institute, School of Medicine, Stanford University, Stanford, California 94305, United States

Monica J. Bohmer[&],

Division of Molecular Microbiology, Burnett School of Biomedical Sciences, University of Central Florida, Orlando, Florida 32826, United States

Jinhua Wang,

Department of Biological Chemistry and Molecular Pharmacology, Harvard Medical School, Boston, Massachusetts 02215, United States; Department of Cancer Biology, Dana-Farber Cancer Institute, Boston, Massachusetts 02215, United States

Flore Nardella,

Division of Molecular Microbiology, Burnett School of Biomedical Sciences, University of Central Florida, Orlando, Florida 32826, United States

Jaeson Calla,

Department of Pediatrics, School of Medicine, University California, San Diego, La Jolla, California 92093, United States

Mariana Laureano De Souza,

Department of Pediatrics, School of Medicine, University California, San Diego, La Jolla, California 92093, United States

Kyra A. Schindler,

Department of Microbiology and Immunology, Columbia University Irving Medical Center, New York, New York 10032, United States

Lukas Montejo,

Corresponding Authors Elizabeth A. Winzeler – Department of Pediatrics, School of Medicine, University California, San Diego, La Jolla, California 92093, United States; ewinzeler@ucsd.edu; **Debopam Chakrabarti** – Division of Molecular Microbiology, Burnett School of Biomedical Sciences, University of Central Florida, Orlando, Florida 32826, United States; dchak@ucf.edu; **Nathanael S. Gray** – Department of Chemical and Systems Biology, ChEM-H, Stanford Cancer Institute, School of Medicine, Stanford University, Stanford, California 94305, United States; nsgray01@stanford.edu.
[&]L.W. and M.J.B. contributed equally to this paper.

Supporting Information

The Supporting Information is available free of charge at <https://pubs.acs.org/doi/10.1021/acs.jmedchem.3c02046>.

LC-MS data for compounds **1–33**. ¹H NMR spectra for compounds **1–33** (PDF)

Molecular formula strings(CSV)

The authors declare the following competing financial interest(s): Nathanael Gray is a founder, science advisory board member (SAB) and equity holder in Syros, C4, Allorion, Lighthorse, Voronoi, Inception, Matchpoint, CobroVentures, GSK, Larkspur (board member), Shenandoah (board member) and Soltego (board member). The Gray lab receives or has received research funding from Novartis, Takeda, Astellas, Taiho, Jansen, Kinogen, Arbell, Deerfield, Springworks, Interline and Sanofi.

●Affiliations for K.A.S., L.M., N.M., and F.R. are those in which the research was conducted.

Division of Molecular Microbiology, Burnett School of Biomedical Sciences, University of Central Florida, Orlando, Florida 32826, United States

Nimisha Mittal,

Department of Pediatrics, School of Medicine, University California, San Diego, La Jolla, California 92093, United States

Frances Rocamora,

Department of Pediatrics, School of Medicine, University California, San Diego, La Jolla, California 92093, United States

Mayland Treat,

School of Public Health, University of California, Berkeley, California 94704, United States

Jordan T. Charlton,

Department of Natural Sciences and Mathematics, Dominican University of California, San Rafael, California 94901, United States

Patrick K. Tumwebaze,

Infectious Disease Research Collaboration, Kampala, Uganda

Philip J. Rosenthal,

Department of Medicine, University of California, San Francisco, California 94110, United States

Roland A. Cooper,

Department of Natural Sciences and Mathematics, Dominican University of California, San Rafael, California 94901, United States

Ratna Chakrabarti,

Division of Cancer Research, Burnett School of Biomedical Sciences, University of Central Florida, Orlando, Florida 32826, United States

Elizabeth A. Winzeler,

Department of Pediatrics, School of Medicine, University California, San Diego, La Jolla, California 92093, United States

Debopam Chakrabarti,

Division of Molecular Microbiology, Burnett School of Biomedical Sciences, University of Central Florida, Orlando, Florida 32826, United States

Nathanael S. Gray

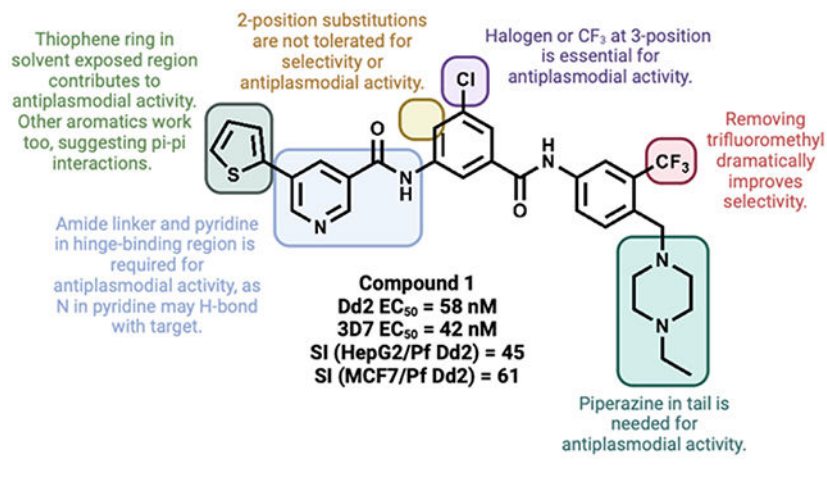
Department of Chemical and Systems Biology, ChEM-H, Stanford Cancer Institute, School of Medicine, Stanford University, Stanford, California 94305, United States

Abstract

While progress has been made in the effort to eradicate malaria, the disease remains a significant threat to global health. Acquired resistance to frontline treatments is emerging in Africa, urging a need for the development of novel antimalarial agents. Repurposing human kinase inhibitors provides a potential expedited route given the availability of a diverse array of kinase-targeting drugs that are approved or in clinical trials. Phenotypic screening of a library of type II human kinase inhibitors identified compound **1** as a lead antimalarial, which was initially developed to

target human ephrin type A receptor 2 (EphA2). Here, we report a structure–activity relationship study and lead optimization of compound **1**, which led to compound **33**, with improved antimalarial activity and selectivity.

Graphical Abstract



INTRODUCTION

Despite significant progress in reducing the global impact of malaria, the mosquito-borne illness caused by parasites of the *Plasmodium* genus remains a threat in many regions, evidenced by an estimated 247 million cases in 2021.¹ One of the most pressing concerns is the emergence of resistance to the frontline treatment, artemisinin-based combination therapy (ACT), in Africa, the region with the most severe burden of malaria.² New antimalarial drugs, ideally directed against novel targets, are needed. A valuable source of novel antimalarials is to repurpose existing compounds originally developed for other therapeutic applications.³ Protein kinase inhibitors are used extensively for the treatment of cancer and are often designed to target mutationally activated kinases.⁴ In addition to oncologic applications, protein kinase inhibitors are utilized in the treatment of a range of other conditions, including ocular hypertension and autoimmune disorders like rheumatoid arthritis and ulcerative colitis.^{4,5} As such, protein kinase inhibitors represent a subset of such compounds that are actively being explored for repurposing as antimalarials.⁶ Protein kinases facilitate myriad parasite functions at every stage of its complex life cycle, and the ability to inhibit multiple stages of the plasmodial life cycle is a key criterion for a lead antimalarial candidate.⁷ Additionally, there is significant divergence between the human and *Plasmodium* kinomes, allowing for selectivity.⁸ Finally, a tremendous amount of research has been conducted in the pursuit of human kinase inhibitors, which can be leveraged to expedite the development of new antiplasmodial inhibitors.⁹⁻¹¹

Most kinase inhibitors are categorized as type I; they act by forming hydrogen bonds to residues in the hinge region of the ATP-binding site, thereby displacing ATP.¹² Type II kinase inhibitors, on the other hand, target the inactive conformation, exploiting a hydrophobic pocket near the ATP binding site generated by a conformational rearrangement

of the activation loop. Type II inhibitors, although possessing a hinge-binding moiety, also contain a hydrophobic tail component, which usually binds to the allosteric pocket beyond the DFG moiety.¹³ The additional interaction with the allosteric pocket influences kinase selectivity and can prolong compound residence time in the binding site, which may augment in vivo efficacy.^{14,15} The type II inhibitors bafetinib, imatinib, and nilotinib are reported to have moderate antimalarial activity, with ring stage EC₅₀s of 1.3, 3.0, and <1 μM, respectively; however, the plasmodial protein target remains unknown.¹⁶ In addition, recently, a new type II pharmacophore was identified as an antiplasmodial agent acting beyond its inhibition of designated kinase *P. falciparum* PK6, although it remains to be seen if the classical type II pharmacophore translated to type II inhibition in *Plasmodium*.¹⁷ Type II kinase inhibitors are an attractive starting point for repurposing for antimalarial activity, given the range of chemical space yet to be explored and the pre-existence of large collections of compounds generated during efforts to target human kinases. In this study, we describe the identification of a type II kinase inhibitor scaffold, exemplified by compound **1**, that displays potent dual-stage antiplasmodial activity in vitro and exhibits efficacy in a mouse malaria model. Our structure–activity analysis revealed an essential role of a 3-position substitution on the central ring in preserving antiplasmodial activity and characterizes the influence of other pharmacophore components on both potency and selectivity.

RESULTS AND DISCUSSION

Identification of Compound **1** as a Lead Antimalarial Agent.

To identify type II scaffolds with the potential to be repurposed as antimalarials, we first conducted a broad phenotypic screen of a type II kinase inhibitor library against the multidrug-resistant Dd2 strain of *P. falciparum*, the most lethal *Plasmodium* species. Asynchronous *P. falciparum* Dd2 blood stage cultures were treated with a 1 μM concentration of compound for 72 h, and growth was assessed by a SYBR Green I-based proliferation assay.¹⁸ Of the library's 553 compounds, 58 inhibited parasite growth by at least 90% at 1 μM (Figure S1). When the EC₅₀s of these compounds were obtained, we identified many compounds with a submicromolar EC₅₀. Among them, thiophenylpyridine compound **1** displayed an EC₅₀ of 80 ± 8 nM in asynchronous cultures. Compound **1** was originally created as part of a series designed to target human EphA2, a receptor tyrosine kinase, in the type II manner.¹⁹ The library included compounds that follow a common pharmacophore: a heterocyclic head, a central ring flanked by linker regions, and a tail that occupies the hydrophobic pocket present in the inactive conformation of EphA2. This potent inhibition of a human kinase raised the concern that, despite promising antiplasmodial action, the utility of compound **1** would be limited because of poor selectivity.

To investigate this possibility, we compared the antiplasmodial activities of four available analogs of compound **1**, which differ only in central ring substitutions in the 2- and 3-positions, for their inhibitory effect on human EphA2, as determined by the SelectScreen Kinase Profiling Service (Invitrogen), an in vitro FRET-based assay. As illustrated in Table 1, substitutions at the 2- and 3-positions in the central ring led to a separation of human EphA2 activity from antiplasmodial activity. Compared to compound **5**, which displays

potent EphA2 inhibition ($IC_{50} = 11$ nM) and poor antiplasmodial activity (Dd2 $EC_{50} = 3.9$ μ M), compound **1** exhibits an almost 900-fold reduction in human EphA2 activity and over 48-fold increase in antiplasmodial activity. To further assess the human kinase selectivity of compound **1**, the binding affinities to a panel of 468 kinases (403 nonmutant kinases) were screened at 1 μ M in the KINOMEscan Profiling Service. As we expected, compound **1** demonstrated outstanding selectivity, with an S (10) selectivity score of 0.035 (Figure S2). These encouraging results suggest that central ring modifications have a crucial role in antiplasmodial activity and that there might be an opportunity to improve selectivity by further modifications to other regions of compound **1**.

Structure–Activity Relationship.

Based on previous SAR studies and molecular modeling, thiophenylpyridine of compound **1** binds to the adenine binding region of the ATP pocket, which is a key determinant of potency and selectivity, and therefore, we focused an initial set of analogs to this region (Table 2). We used both the multidrug-resistant *P. falciparum* Dd2 and the drug-sensitive *P. falciparum* 3D7 strains to test compounds against ring-stage malaria parasites, and an MTS-based cell proliferation assay in the human hepatocarcinoma line HepG2 and the adenocarcinoma line MCF7 for general cytotoxicity and selectivity. We first removed the thiophene, leading to a pyridine compound **6**, which resulted in a 3-fold weaker potency than compound **1**, accompanied by marginal improvement in selectivity (indices of 71 and 75). To better understand the effect of the pyridine substitution, analogs with piperazine (compound **7**), phenyl group (compound **8**), phenylthiophene (compound **9**), pyrimidine (compound **10**), pyrimidin-2-amine (compound **11**), and nicotinonitrile (compound **12**) were synthesized. Antiplasmodial activity evaluation demonstrated that replacing the pyridine with a saturated piperazine ring (**7**) resulted in the loss of potency (EC_{50} 1.2 μ M) and selectivity. Removing the nitrogen from pyridine (compound **8**) and thiophenylpyridine (compound **9**) resulted in a further decrease in the potency by 4- to 5-fold, indicating that the pyridine is essential for antiplasmodial activity, and the nitrogen in the pyridine ring may contribute to hydrogen-bonding with the potential target. Introducing small substitution groups and/or additional nitrogen atoms to the pyridine ring (compound **10**, compound **11**, compound **12**) did not rescue the potency and selectivity from compounds **8** and **9**. This implies that the thiophene ring is a major contributor to antimalarial activity, suggesting a π - π interaction between the thiophene and the potential target might exist. Furan (compound **13**), phenyl (compound **14**), thiazole (compound **15**), and benzonitrile (compound **16**) were employed to further probe into the potency-enhancing effect of thiophene. As a result, compounds **13**, **14**, **15**, and **16** exhibited comparable antimalarial activity, and interestingly, compounds **13** and **15** displayed improved selectivity compared to compound **1**. Compound **16** stood out as the most potent analog in this series, with an EC_{50} of 36 nM against both the Dd2 and 3D7 strains.

Next, we focused on the amide portions of the molecule (Table 3). We observed previously that the amide close to thiophenylpyridine is essential for potent inhibition of EphA2. Removal or replacement of the carbonyl group with methylene led to a 6-fold loss of potency (**17** and **18**). Reversing the amide bonds did not improve the potency (**19** and **20**). The tail on compound **1**, trifluoromethyl ($-CF_3$) and piperazine, was positioned to

the pocket created by the movement of the activation loop. Truncating the piperazine significantly decreased the potency, with an EC₅₀ of 1110 nM for compound **21**. Removal of the CF₃ (**22**) retained the activity but, more importantly, dramatically improved the selectivity. Incorporation of smaller type II tail 4-(pyridin-2-yl) morpho-line decreased potency by 13-fold (compound **23**).

After exploring the hinge region, amide linker, and tail parts, we shifted our focus to the central ring. Encouraged by the preliminary SAR results (Table 1), it was clear that the modification of the central ring provided us with a decent point for further SAR exploration. As shown in Table 4, the EC₅₀ of compound **1** was 2.59 μM in HepG2 and 3.51 μM in MCF7, producing respectable selectivity indices of 45 and 61, respectively. Replacement of the 3-Cl group with 2-F (compound **24**) and 2-OMe (compound **25**) dramatically reduced the activity and selectivity. Installing the F to the 4-position, affording compound **26**, slightly inhibited *Plasmodium* (EC₅₀ = 867 nM) with poor selectivity. Introducing F to the 4-position combined with the addition of a methyl substitution at the 2-position (compound **27**) led to sharply weakened antiplasmodial activity and selectivity, which indicates that 2-position substitution is not tolerated for maintaining antimalarial activity and selectivity. Engagement of a methyl group to the 3-position, affording compound **28**, showed similar potency with compound **2** (Table 1), 6-fold less potent than compound **1**. To further investigate the effects of the central ring, the phenyl ring was replaced by pyridine, generating compounds **29** and **30**. The positions of a nitrogen atom in pyridine exerted a dramatic effect on antiplasmodial potency and selectivity. Moving the nitrogen atom from the *ortho* position (compound **29**) to the *meta* position (compound **30**) led to a more than 7-fold improvement in both potency and selectivity, which proved our speculation that 2-position substitution is not tolerated, and 3-substitution is essential for antimalarial activity. Combined with the above SAR data, these results demonstrated that 3-position substitutions are important for potency, and the 3-Cl substitution displayed the highest potency. The excellent potency of 3-Cl substitution may be attributed to halogen bonding and/or hydrophobic interactions with the potential targets.²⁰⁻²² To verify our hypothesis, 3-Cl was replaced by 3-F (**31**), 3-Br (**32**), and 3-CF₃ (**33**). As we expected, all three of these inhibitors demonstrated similar antiplasmodial activity compared to compound **1**, in which compound **33** slightly outperformed on potency (EC₅₀: 31 nM for Dd2, 35 nM for 3D7) and demonstrated boosted selectivity (indices of 92 and 114).

In Vitro Metabolic Stability and In Vivo Pharmacokinetics.

Given the potent activity of compound **1** and its analogs, we evaluated all the active compounds with EC₅₀ below 150 nM for their stability in mouse microsomes. As shown in Table 5, compounds **1**, **13–16**, **22**, **32**, and **33** exhibit suitable microsomal stability and low clearance, compound **1** being the most stable. By contrast, compounds **6** and **30** are metabolized rapidly/have a fast clearance.

As aforementioned, compound **1** demonstrated the best metabolic stability. To prove the antimalarial efficacy of this scaffold, compound **1** was selected for further in vivo studies. Pharmacokinetic studies of compound **1** in mice are shown in Table 6: it exhibits low bioavailability (4.8%) after oral administration, which may be attributed to its poor solubility and cell permeability (Table S1), leading to slow absorption (T_{\max} = 4.67 h). Intravenously,

compound **1** displayed a short half-life (4.16 h) and a moderate exposure level (volume of distribution 0.84 L/kg), indicating low penetration into tissues. By comparison, the known antiplasmodial compound GNF179 displays a half-life of 8.9 h and a volume of distribution of 11.8 L/kg.²³ Scaffold optimization efforts are presently underway to improve metabolic stability and pharmacokinetic properties while retaining high potency and selectivity.

Compound 1 Displays Both Prophylactic and Therapeutic Efficacy In Vivo.

To determine whether compound **1** possesses the coveted multistage activity present in a lead antimalarial candidate, we evaluated its activity against the liver stage. A liver stage assay utilizing luciferase-expressing *P. berghei* parasites (*P. berghei*^{Luc}) revealed an EC₅₀ of 1.77 ± 0.07 μM (Figure S3). We then evaluated the in vivo efficacy of compound **1** when administered prophylactically and therapeutically. In the prophylactic model, the compound was administered IV as a single dose, 6 h before IV inoculation with *P. berghei*^{Luc} sporozoites.²³ The therapeutic model utilized the standard 4-day Peter's test, in which the mice are infected IP with *P. berghei*^{Luc} infected red blood cells (iRBCs) and treated IV, once daily, for 4 days.²⁴ Infection was monitored by flow cytometry and by in vivo imaging (Figure S4).²⁵ Both experimental models were conducted utilizing two drug doses, 15 and 50 mg/kg IV, and as a control, we used an antiplasmodial compound with both blood and liver stage activity, GNF179.²³ For this proof-of-concept experiment, although not ideal for antimalarial, we used the IV route of administration. In both sets of experiments, by day 12, parasitemia was systemic and widespread in untreated control groups (Figures 1 and S4). When compound **1** was used prophylactically at 15 or 50 mg/kg, mice cleared the infection and showed no recrudescence until sacrifice at 90 days (Figure 1A,C). Similarly, the mice treated therapeutically with 15 mg/kg were cured of infection (Figure 1B,D). The mice treated prophylactically with the lower dose, did show a very weak indication of infection at the injection site, detected by luminescence (Figure S4) on day 2, though parasitemia measurements on day 6 and onward showed no evidence of infection (Figure 1A). We attribute the early luciferase signal to sporozoites being retained at the injection site, potentially in the skin. Taken together, these results indicated that, in the murine model, compound **1** acted both therapeutically, by resolving blood stage infection, and prophylactically, by preventing the establishment of a systemic infection, even at a dose as low as 15 mg/kg.

Compound 1 Kills Parasites Rapidly and Targets Ring Stages More Effectively.

Having established the efficacy of compound **1** in vivo, in-depth characterization of the effects of compound **1** on blood-stage *P. falciparum* was conducted to evaluate its properties as an antimalarial lead candidate. The rate of parasiticidal activity was evaluated using a flow cytometry-based assay, in which asynchronous Dd2 cultures were treated for 12, 24, or 48 h with 10 × EC₅₀ of compound **1**, washed, and monitored for 4 days. As shown in Figure 2A, parasites treated with compound **1** for as little as 12 h failed to recover within 4 days. To dissect the parasite clearance kinetics precisely, a parasite reduction ratio assay was performed with both compound **1** and the potent antiplasmodial analog, compound **16**.²⁶ Synchronized parasites were exposed to 10 × EC₅₀ of the compound at ring stage, and every 24 h for 120 h, an aliquot of the culture was washed and serially diluted in uninfected red blood cells, and growth was assessed after 21 days. As shown in Figure 2D, both compound

1 and compound **16** are fast-acting, similar to dihydroartemisinin (DHA), with no lag phase detected and a 99.9% parasite clearance time (PCT) of less than 32 h.

We then sought to identify the stage at which the compound exerted its maximum antimalarial effects through a stage-specific assay. Synchronized Dd2 culture was treated with $5 \times \text{EC}_{50}$ of compound **1** at 6-, 18-, 30-, and 42 h post-invasion (HPI) and monitored until 54 HPI by microscopy and flow cytometry, staining with YOYO-1 for nuclear content. As shown in Figure 3, the histograms in the control reflect a rightward shift in the YOYO-1 peak due to an increase in DNA through schizogony, followed by a leftward peak for reinvasion at 54 h. However, when compound **1** was added at 6 HPI, this early peak failed to shift, and microscopy showed that parasites seemed to remain stunted in the ring stage. When applied at both 18 and 30 HPI, there was a delayed shift, and parasites were clearly malformed. However, by 42 HPI, the effect was much less pronounced. A reinvasion peak was observed, indicating the production of viable merozoites and successful reinvasion, though some parasites still displayed aberrant morphology.

Finally, to quantitatively evaluate the varying susceptibility of parasites through the life cycle to compound **1**, we treated highly synchronized (0–3 HPI) 3D7 parasites at four points in the asexual life cycle (6, 16, 26, and 36 HPI), and after 72 h performed a SYBR Green I-based proliferation assay to obtain EC_{50} values. We found that compound **1** exhibited a notably lower EC_{50} in the early ring stage (30 nM) that increased throughout the lifecycle to 80 nM at 36 HPI (Figure 3E).

Compound 1 and Compound 16 are Effective against Artemisinin-Resistant Clinical Isolates.

The evidence that compound **1** is fast-acting, primarily in the ring stage, raised the concern that the compound acts in a manner similar to artemisinin, and may therefore be vulnerable to emerging artemisinin resistance.²⁷ To evaluate the effect of compound **1** and compound **16** on artemisinin-resistant *P. falciparum* parasites, we assessed the ring stage survival of field isolates that are resistant to artemisinin and piperazine (PPQ), an analog of chloroquine that is used in an ACT. Three strains from Cambodia were used: one that remains sensitive to artemisinin (IPC 5188), one that is artemisinin-resistant (IPC 5202), and one that is both artemisinin- and piperazine-resistant (IPC 6261).²⁸⁻³² Using the ring stage survival assay (RSA),²⁹ highly synchronized early ring stage parasites (0–3 HPI) were treated with $10 \times \text{EC}_{50}$ of compound **1** or compound **16** for 6 h before compound removal, and survival was evaluated at 72 h with Giemsa-stained thin blood smears. As controls, DHA and the vehicle, DMSO, were used. As shown in Figure 4A, compound **1** and compound **16** displayed a similar inhibitory profile to each other in all strains, which would be expected for analogs. However, the survival in all strains, including 3D7, was notably higher than that of the DHA-treated cultures, indicating that 6-h incubation might not be sufficient to exert a maximal effect. We then performed a piperazine survival assay (PSA).³¹ This assay is identical to the RSA with the exception that piperazine (PPQ) served as the control, and the treatment duration is 48 h. In this assay, the parasites treated with either compound **1** or compound **16**, regardless of strain, did not survive the 48 h treatment (Figure 4B). Furthermore, the EC_{50} values of both compounds remained in the

low nanomolar range in all strains (Figure 4C). Taken together, these results indicate that compound **1** and compound **16** maintain efficacy against both artemisinin and piperazine-resistant strains, though a treatment time of between 6 and 48 h is required.

Compound **1** Maintains Potency in Ex Vivo Ugandan Isolates.

We then evaluated the efficacy of compound **1** in currently circulating parasite populations. Ex vivo *P. falciparum* isolates were obtained from patients from three locations in northern and eastern Uganda: The Patongo Health Center in Patongo, Agago District; the Tororo District Hospital in Tororo, Tororo District, and the Busiu Health Center in Busiu, Mbale District. Activity, evaluated with the SYBR-Green I proliferation assay, was compared to *P. falciparum* Dd2 and *P. falciparum* 3D7 parasites in predominantly ring stage to reflect the stage of the clinical isolates more closely. As shown in Figure 5, Compound **1** maintained very potent activity against all ex vivo isolates, with an average EC₅₀ of 9.21 nM. This suggests that prevailing *P. falciparum* populations in eastern and northern Uganda lack a genetic background that would reduce compound **1** efficacy, underscoring the compound's utility as a preclinical candidate.

Compound **1** Maintains Potency in Strains Resistant to Known Antiplasmodials.

Finally, we evaluated the cross-resistance of compound **1** in *P. falciparum* strains possessing resistance-conferring mutations to antimalarial drug candidates. The purpose of this was 2-fold; cross-resistance would suggest a possible mechanism of action, as well as indicate a looming risk of resistance. The efficacy of compound **1** was assessed against three *P. falciparum* lines with resistance-causing mutations in the following genes: AcAS, CARL, and PI4K. The line AcAS A597 V has a mutation within the acetyl-coenzyme A synthetase (PF3D7_0627800) which renders parasites resistant to the compound MMV084978, a promising antiplasmodial compound in development.³³ CARL I1139K has a mutation in the cyclic amine resistance locus (PF3D7_0321900), providing resistance to imidazolopiperazine antiplasmodials like GNF179.³⁴ PI4K S1320L contains a mutation in the phosphatidylinositol 4-kinase (PF3D7_0509800), conferring resistance to imidazopyrazines such as KDU691.³⁵ As controls, the compounds associated with resistance in the mutants were used, as well as artemisinin. As shown in Figure 6, there was no difference between compound **1** EC₅₀ among the three resistant lines.

Compound **1** Is Irresistible to Drug Selection in *P. falciparum* In Vitro.

To ascertain a mechanism of action, we attempted to generate a resistant line, with the aim of creating clonal populations of resistant parasites. The genomes of the resistant clones would then be sequenced and compared to the parental line to identify resistance-conferring single nucleotide polymorphisms (SNPs) or gene duplication events, possibly revealing causal targets.³⁶ The *P. falciparum* clonal line, Dd2-B2, was used for resistance line generation.³⁷ Three flasks containing 1×10^8 blood stage Dd2-B2 parasites were treated with $1 \times$ EC₅₀ of compound **1** until death was observed, and one flask of equal parasitemia was left untreated (Figure S5). Flasks 2 and 3 failed to recover after the compound was removed. Only one flask achieved weak resistance, intermittently tolerating $2 \times$ EC₅₀ of compound **1**. However, after the second pulse of treatment at this concentration, the

parasites failed to rebound, suggesting that the compound kills in a manner that is not easily overcome by genetic mutation. While this hampered our target identification efforts, it also underscored the value of this compound, as one of the strongest exclusion criteria for a prospective antiplasmodial drug is the propensity to develop resistance.

To confirm the “irresistibility” of compound **1**, we determined the minimum inoculum of resistance (MIR), a metric used to evaluate the risk of an antiplasmodial compound for inducing resistance.²⁶ The EC₅₀ and EC₁₀ were determined in the Dd2-B2 strain (40.6 and 53.4 nM, respectively) using a flow cytometry-based method on ring-stage parasites. Subsequently, two selections were conducted, one with 1.4×10^7 parasites (1.2×10^6 parasites in 12 wells), and another with 3×10^7 parasites (1×10^7 parasites in 3 wells). After continuous treatment with $3 \times \text{EC}_{10}$ of compound **1**, cultures were monitored thrice weekly via thin blood smear. After treatment, parasites were cleared from the culture quickly and failed to recover within 50 days, indicating that compound **1** has an MIR of >7 and a high barrier to resistance.⁷ While compound **1** shows clear promise as an antimalarial due to its dual therapeutic/prophylactic potential, the cellular mechanism of action remains elusive. The fact that we were unable to generate resistance lines through two different approaches bodes well for the compound as a treatment option; however, the lack of resistant clones obliges us to use other methods for target identification, and these efforts are presently underway.

CONCLUSIONS

A phenotypic screen of a type II library yielded compound **1** with potent antiplasmodial activity in both the asexual blood and liver stages, which was manifested as in vivo efficacy when applied as both a therapeutic and prophylactic. Through extensive structure–activity relationship analysis of its analogs, we deconvoluted the important components of compound **1**. The 2-position in the central ring is found to be essential to both selectivity and antimalarial potency, as substitutions at this location are not tolerated; rather, 2-substitution is associated with increased activity against human EphA2. In the 3-position of the central ring, a substitution group, especially a trifluoromethyl group or a halogen is essential for potency. This potency is accentuated by the addition of an additional aromatic moiety to the solvent-exposed region. In addition, the linker and tail portions also influence potency and selectivity: an amide linker adjoining the head region is required for potency, and a reduced type II tail, lacking the trifluoromethyl group improves selectivity. Optimization of the scaffold continues, with the aim of improving pharmacokinetic properties and advancing a lead compound with potential as a preclinical antimalarial candidate.

In addition to gaining valuable structure–activity insight into this scaffold, we also characterized its antiplasmodial activity, thereby evaluating its potential as a lead antimalarial. We found that compound **1** is a fast-acting parasitocidal agent in the asexual blood stages of *P. falciparum*, and this efficacy extends to strains resistant to current and candidate antimalarials, as well as in *ex vivo* isolates. Additionally, compound **1** displays promising activity in the liver stage and is efficacious in vivo when applied therapeutically or prophylactically, underscoring its dual-stage utility. Finally, we demonstrated that compound **1** is “irresistible,” failing to generate resistance in two separate attempts. Notably,

compound **1** provides the platform to meet Medicines for Malaria Venture's target candidate profiles because of its therapeutic and prophylactic activities.

While compound **1** was designed as a type II protein kinase inhibitor, it remains to be determined whether the compound inhibits a plasmodial or host kinase, or if it inhibits in a type II fashion. Indeed, it is not unusual for the kinase inhibitors that exert their therapeutic effects via "off-targets," particularly bromodomain-containing proteins or tubulin.³⁸ Target identification is underway to deconvolute the mechanism of action of compound **1**.

CHEMISTRY

Synthetic routes for the preparation of compounds are outlined in Schemes 1-3. The synthesis of derivatives **1**, **6**, **8–16** commenced with the known commercially available 4-((4-Methylpiperazin-1-yl)methyl)-3-(trifluoromethyl)aniline, which underwent HATU-mediated condensation with benzoic acid derivatives to generate amide **S2**. Reduction of the resulting nitro compound as aniline analogs followed by a second condensation reaction furnished final products (Scheme 1). Derivatives **7**, **17–23** were synthesized based on the synthetic routes described in Scheme 2. With **S3** in hand, treatment of **S3** with triphosgene provided the active intermediate, which was subject to a condensation reaction with 1-methylpiperazine to afford **7**. Analogs **17** and **18** were synthesized from **S3** through reductive amination and Pd-mediated amination coupling, respectively. Derivatives **19–23** were prepared in a three-step sequence involving (1) HATU-mediated condensation; (2) Fe-induced reduction of the resulting nitro intermediate; (3) Amide formation of the resulting aniline with 5-(thiophene-2-yl) nicotinoyl chloride. Compounds **2–5**, and **24–33** were prepared via similar synthetic routes (Scheme 3). HATU-mediated condensation of **S1** with various nitrobenzoic acids gave intermediate **S11** and subsequent reduction of resulting nitro compounds and amide formation with nicotinic acid derivatives generating the desired final products.

EXPERIMENTAL SECTION

Compound Synthesis.

Starting materials, reagents, and solvents were purchased from commercial suppliers and were used without further purification unless otherwise noted. All reactions were monitored using a Waters Acquity UPLC/MS system (Waters PDA e λ Detector, QDa Detector, Sample manager - FL, Binary Solvent Manager) using Acquity UPLC BEH C18 column (2.1 \times 50 mm, 1.7 μ m particle size): solvent gradient = 85% A at 0 min, 1% A at 1.7 min; solvent A = 0.1% formic acid in water; solvent B = 0.1% formic acid in Acetonitrile; flow rate: 0.6 mL/min. Reaction products were purified by flash column chromatography using CombiFlashRf with Teledyne Isco RediSep normal-phase silica flash columns (4, 12, 24, 40 or 80 g) and a Waters HPLC system using a SunFireTM Prep C18 column (19 \times 100 mm, 5 μ m particle size): solvent gradient = 80% A at 0 min, 10% A at 25 min; solvent A = 0.035% TFA in Water; solvent B = 0.035% TFA in MeOH; flow rate: 25 mL/min. ¹H NMR spectra were recorded on 500 MHz Bruker Avance III spectrometers, and ¹³C NMR spectra were recorded on a 125 MHz Bruker Avance III spectrometer. Chemical shifts are reported in parts per million (ppm, δ) downfield from tetramethylsilane (TMS). Coupling constants

(*J*) are reported in Hz. Spin multiplicities are described as *br* (broad), *s* (singlet), *d* (doublet), *t* (triplet), *q* (quartet), and *m* (multiplet). Purities of assayed compounds were in all cases greater than 95%, as determined by reverse-phase LC–MS analysis. The LC–MS traces and ¹H NMR spectra have been provided in Figures S6 and S7, respectively

General Procedure A for Preparation of Compounds 1, 6, 8–16. Step 1: To a solution of **S1** (4.00 g, 13.9 mmol, 1.0 equiv) in DCM (28 mL) were added 3-chloro-5-nitrobenzoic acid (3.15 g, 14.3 mmol, 1.03 equiv) and DIPEA (1.98 g, 15.3 mmol, 2.67 mL, 1.1 equiv) at 0 °C. The mixture was stirred at 25 °C for 0.5 h. LC–MS showed that **S1** was consumed completely and one main peak with desired MS was detected. The reaction mixture was poured into water (15 mL) and the reaction was extracted with DCM (50 mL, 30 mL). The organic phase was dried over Na₂SO₄ and filtered under reduced pressure to give **S2** (4.2 g, 8.92 mmol, 64.1% yield) as a white solid. ¹H NMR (400 MHz, CD₃OD) δ 8.77 (s, 1H), 8.49 (s, 1H), 8.40 (s, 1H), 8.16 (s, 1H), 8.02 (d, *J* = 8.4 Hz, 1H), 7.80 (d, *J* = 8.4 Hz, 1H), 3.78 (s, 2H), 2.25–3.24 (m, 10H) 1.35 (t, *J* = 7.6 Hz, 3H).

Step 2: To a solution of **S2** (2.50 g, 5.31 mmol, 1.0 equiv) in EtOH (12 mL) and H₂O (4.0 mL) were added NH₄Cl (852 mg, 15.9 mmol, 3.0 equiv) and Fe (1.48 g, 26.6 mmol, 5.0 equiv) at 25 °C. The mixture was stirred at 80 °C for 5 h. TLC (DCM: MeOH = 0:1, Product *R*_f = 0.12) indicated **S2** was consumed completely one new spot formed. The reaction was clean according to TLC. The reaction mixture was filtered and concentrated under reduced pressure to remove EtOH. The reaction mixture was poured into water (15 mL) and extracted with ethyl acetate (50 mL, 30 mL). The combined organic phase was washed with saturated brine (10 mL), dried over Na₂SO₄, filtered, and concentrated in a vacuum to give **S3** (2 g, 4.54 mmol, 85.4% yield) as a white solid. ¹H NMR (400 MHz, DMSO-*d*₆) δ 10.45 (s, 1H), 8.18 (d, *J* = 2.0 Hz, 1H), 8.06 (d, *J* = 8.4 Hz, 1H), 7.70 (d, *J* = 8.4 Hz, 1H), 7.04–7.10 (m, 2H), 6.79 (t, *J* = 2.0 Hz, 1H), 5.72 (s, 2H), 3.65 (s, 2H), 2.75–3.17 (m, 10H), 1.21 (t, *J* = 7.2 Hz, 3H).

Step 3: Acid chloride way: nicotinic acid derivatives (0.15 mmol) were dissolved in SOCl₂ (2 mL) at 25 °C. The mixture was stirred at 80 °C for 2 h. Then, the reaction mixture was concentrated under reduced pressure to remove SOCl₂ to give acid chloride as a yellow solid, which was put into the next step directly. A solution of **S3** (0.1 mmol, 1.0 equiv) in DMF (2 mL) was added above acid chloride (0.15 mmol, 1.5 equiv) and DIPEA (0.3 mmol, 3.0 equiv) at 0 °C. The mixture was stirred at 25 °C for 30 min. LC–MS showed that **S3** was consumed completely and one main peak with the desired MS was detected. The reaction mixture was poured into water (15 mL) and the reaction was extracted with ethyl acetate (50 mL, 30 mL). The reaction mixture was dried over Na₂SO₄, filtered, and concentrated under reduced pressure to give a residue. The residue was purified by prep-HPLC to give the final compounds.

HATU-mediated amide formation way: To a solution of **S3** (0.10 mmol, 1.0 equiv) and nicotinic acid analogs (0.15 mmol, 1.5 equiv) in DMF (2 mL), 1-[bis(dimethylamino)-methylene]-1H-1,2,3-triazolo[4,5-*b*]pyridinium 3-oxide hexafluorophosphate (HATU) (76 mg, 0.20 mmol, 2.0 equiv) and N,N-diisopropylethylamine (DIPEA) (64 mg, 0.50 mmol, 5.0 equiv) were added at 0 °C. This mixture then was stirred at 25 °C for 12 h. LC–MS showed

that **S3** was consumed completely and one main peak with the desired MS was detected. The reaction mixture was poured into water (15 mL) and was extracted with ethyl acetate (3 × 50 mL). The reaction mixture was then dried over Na₂SO₄, filtered, and concentrated under reduced pressure to give a residue. The residue was purified by preparative HPLC to give the final compounds.

N-(3-Chloro-5-((4-((4-ethylpiperazin-1-yl)methyl)-3-(trifluoromethyl)phenyl)carbamoyl)phenyl)-5-(thiophen-2-yl)nicotinamide (Compound 1).—The title compound was

prepared according to the general procedure acid chloride pathway. ¹H NMR (400 MHz, DMSO-*d*₆): δ (ppm): 10.87 (s, 1H), 10.64 (s, 1H), 9.12 (d, *J* = 2.4, 1H), 9.03 (d, *J* = 2.0 Hz, 1H), 8.53 (t, *J* = 2.0 Hz, 1H), 8.27 (t, *J* = 1.6 Hz, 1H), 8.22 (t, *J* = 2.0 Hz, 1H), 8.18 (d, *J* = 2.0 Hz, 1H), 8.04–8.07 (m, 1H), 7.86 (t, *J* = 1.6 Hz, 1H), 7.79 (dd, *J* = 3.6, 0.8 Hz, 1H), 7.72–7.75 (m, 2H), 7.24–7.27 (m, 1H), 3.57 (s, 2H), 2.29–2.40 (m, 10H), 0.98 (t, *J* = 7.2 Hz, 3H).

Synthesis of Compound **1**, hydrochloride salt. A solution of Compound **1** (1.60 g, 2.55 mmol, 1.0 equiv) in H₂O (5 mL) and HCl (0.5 M, 20.4 mL, 4.0 equiv) was stirred at 25 °C for 30 min. The solution then was lyophilized to give compound **1** (1.05 g, 1.42 mmol, 55.8% yield, HCl). ¹H NMR (500 MHz, DMSO-*d*₆) δ 11.22 (s, 1H), 10.93 (s, 1H), 9.19 (d, *J* = 2.2 Hz, 1H), 9.14 (d, *J* = 2.0 Hz, 1H), 8.78 (t, *J* = 2.1 Hz, 1H), 8.40 (t, *J* = 1.7 Hz, 1H), 8.38–8.34 (m, 1H), 8.30 (t, *J* = 1.9 Hz, 1H), 8.28–8.18 (m, 2H), 7.94 (t, *J* = 1.7 Hz, 1H), 7.91 (dd, *J* = 3.6, 1.2 Hz, 1H), 7.79 (dd, *J* = 5.1, 1.1 Hz, 1H), 7.29 (dd, *J* = 5.1, 3.6 Hz, 1H), 4.37–4.34 (m, 2H), 3.68 (d, *J* = 12.0 Hz, 2H), 3.46 (s, 6H), 3.20 (d, *J* = 8.9 Hz, 2H), 1.29 (t, *J* = 7.3 Hz, 3H). ¹³C NMR (125 MHz, DMSO-*D*₆) δ 164.98, 164.10, 147.76, 146.66, 140.89, 140.41, 138.55, 136.96, 134.20, 133.63, 133.56, 131.08, 130.58, 129.39, 128.62, 127.08, 125.35, 124.03, 123.44, 123.17, 123.14, 119.25, 118.01, 117.96, 55.70, 50.98, 48.79, 48.24, 9.18. MS (ESI): calcd. for C₃₁H₃₀ClF₃N₅O₂S⁺ [M + H]⁺ 628.18, found 628.01.

N-(3-(4-(4-Ethylpiperazin-1-yl)methyl)-3-(trifluoromethyl)-phenyl)carbamoyl)-5-methoxyphenyl)-5-(thiophen-2-yl) nicotinamide (Compound 2).—The title compound was prepared according to the general procedure acid chloride pathway. ¹H NMR (500 MHz, DMSO-*d*₆) δ 10.80 (s, 1H), 10.65 (s, 1H), 9.17 (s, 1H), 9.10 (s, 1H), 8.59 (t, *J* = 2.1 Hz, 1H), 8.27 (d, *J* = 2.2 Hz, 1H), 8.17 (dd, *J* = 8.5, 2.2 Hz, 1H), 8.03 (d, *J* = 1.7 Hz, 1H), 7.85 (dd, *J* = 3.6, 1.2 Hz, 1H), 7.79 (ddd, *J* = 9.3, 4.6, 1.6 Hz, 3H), 7.42–7.37 (m, 1H), 7.34–7.29 (m, 1H), 3.94 (s, 3H), 3.76 (s, 2H), 3.51–3.43 (m, 2H), 3.25–3.13 (m, 2H), 3.12–3.03 (m, 2H), 3.00 (d, *J* = 13.2 Hz, 2H), 2.49 (t, *J* = 12.3 Hz, 2H), 1.28 (t, *J* = 7.3 Hz, 3H). (ESI): calcd. for C₃₂H₃₃F₃N₅O₃S⁺ [M + H]⁺ 624.23, found 624.21.

N-(3-((4-((4-Ethylpiperazin-1-yl)methyl)-3-(trifluoromethyl)phenyl)carbamoyl)phenyl)-5-(thiophen-2-yl)nicotinamide (Compound 3).—The title compound was prepared

according to the general procedure acid chloride pathway. ¹H NMR (500 MHz, DMSO-*d*₆) δ 10.82 (s, 1H), 10.68 (s, 1H), 9.17 (d, *J* = 2.2 Hz, 1H), 9.10 (d, *J* = 2.1 Hz, 1H), 8.59 (t, *J* = 2.2 Hz, 1H), 8.43 (t, *J* = 2.0 Hz, 1H), 8.29 (d, *J* = 2.2 Hz, 1H), 8.17 (dd, *J* = 8.4, 2.2 Hz, 1H), 8.08 (dd, *J* = 7.8, 2.2 Hz, 1H), 7.85 (dd, *J* = 3.6, 1.2 Hz, 1H), 7.82 (dt, *J* = 7.9, 1.2 Hz,

1H), 7.81–7.78 (m, 2H), 7.64 (t, $J = 7.9$ Hz, 1H), 7.32 (dd, $J = 5.1, 3.6$ Hz, 1H), 3.76 (s, 2H), 3.60–3.45 (m, 2H), 3.21 (q, $J = 7.3$ Hz, 2H), 3.07–2.98 (m, 4H), 2.46 (t, $J = 12.5$ Hz, 2H), 1.27 (t, $J = 7.3$ Hz, 3H). (ESI): calcd. for $C_{31}H_{31}F_3N_5O_2S^+$ $[M + H]^+$ 594.21, found 594.16.

N-(2-Chloro-5-((4-((4-ethylpiperazin-1-yl)methyl)-3-(trifluoromethyl)phenyl)carbamoyl)phenyl)-5-(thiophen-2-yl)nicotinamide (Compound 4).—The title compound

was prepared according to the general procedure acid chloride pathway. 1H NMR (500 MHz, DMSO- d_6) δ 10.65 (s, 1H), 10.64 (s, 1H), 9.13 (d, $J = 2.3$ Hz, 1H), 9.05 (d, $J = 2.0$ Hz, 1H), 8.55 (t, $J = 2.2$ Hz, 1H), 8.20 (dd, $J = 11.8, 2.2$ Hz, 2H), 8.10 (dd, $J = 8.6, 2.2$ Hz, 1H), 7.95 (dd, $J = 8.4, 2.2$ Hz, 1H), 7.83–7.76 (m, 2H), 7.75–7.69 (m, 2H), 7.24 (dd, $J = 5.1, 3.6$ Hz, 1H), 3.69 (s, 2H), 3.45 (d, $J = 12.0$ Hz, 2H), 3.13 (q, $J = 7.3$ Hz, 2H), 3.05–2.96 (m, 2H), 2.93 (d, $J = 13.9$ Hz, 2H), 2.41 (t, $J = 12.2$ Hz, 2H), 1.20 (t, $J = 7.3$ Hz, 4H). (ESI): calcd. for $C_{31}H_{30}ClF_3N_5O_2S^+$ $[M + H]^+$ 628.18, found 628.11.

N-(5-((4-((4-Ethylpiperazin-1-yl)methyl)-3-(trifluoromethyl)phenyl)carbamoyl)-2-methylphenyl)-5-(thiophen-2-yl)nicotinamide (Compound 5).—The title

compound was prepared according to the general procedure acid chloride pathway. 1H NMR (500 MHz, DMSO- d_6) δ 10.53 (s, 1H), 10.39 (s, 1H), 9.14 (d, $J = 2.2$ Hz, 1H), 9.07 (d, $J = 2.0$ Hz, 1H), 8.56 (t, $J = 2.2$ Hz, 1H), 8.23 (d, $J = 2.2$ Hz, 1H), 8.14 (dd, $J = 8.5, 2.2$ Hz, 1H), 8.05 (d, $J = 1.9$ Hz, 1H), 7.87 (dd, $J = 8.0, 1.9$ Hz, 1H), 7.80 (dd, $J = 3.7, 1.2$ Hz, 1H), 7.75 (dd, $J = 5.1, 1.2$ Hz, 1H), 7.73 (d, $J = 8.6$ Hz, 1H), 7.51 (d, $J = 8.1$ Hz, 1H), 7.26 (dd, $J = 5.1, 3.6$ Hz, 1H), 3.70 (s, 2H), 3.47 (d, $J = 12.0$ Hz, 2H), 3.16 (q, $J = 7.3$ Hz, 2H), 3.04–2.93 (m, 4H), 2.41 (d, $J = 12.3$ Hz, 2H), 2.37 (s, 3H), 1.22 (t, $J = 7.3$ Hz, 3H). (ESI): calcd. for $C_{32}H_{33}F_3N_5O_2S^+$ $[M + H]^+$ 608.23, found 608.21.

N-(3-Chloro-5-((4-((4-ethylpiperazin-1-yl)methyl)-3-(trifluoromethyl)phenyl)carbamoyl)phenyl)nicotinamide (Compound 6).—The title compound was

prepared according to the general procedure HATU-mediated amide formation pathway. White powder (28 mg, 51%). 1H NMR (500 MHz, DMSO- d_6) δ 10.83 (s, 1H), 10.67 (s, 1H), 9.16 (d, $J = 2.3$ Hz, 1H), 8.82 (dd, $J = 4.8, 1.7$ Hz, 1H), 8.36 (dt, $J = 8.0, 2.0$ Hz, 1H), 8.31 (t, $J = 1.8$ Hz, 1H), 8.22–8.16 (m, 2H), 8.11 (dd, $J = 8.4, 2.2$ Hz, 1H), 7.84 (t, $J = 1.8$ Hz, 1H), 7.75 (d, $J = 8.5$ Hz, 1H), 7.63 (dd, $J = 8.0, 4.9$ Hz, 1H), 3.71 (s, 2H), 3.47 (d, $J = 12.0$ Hz, 2H), 3.16 (q, $J = 7.4$ Hz, 2H), 3.08–2.90 (m, 4H), 2.41 (d, $J = 12.2$ Hz, 2H), 1.22 (t, $J = 7.3$ Hz, 3H). (ESI): calcd. for $C_{27}H_{28}ClF_3N_5O_2^+$ $[M + H]^+$ 546.19, found 546.23.

N-(3-Chloro-5-((4-((4-ethylpiperazin-1-yl)methyl)-3-(trifluoromethyl)phenyl)carbamoyl)phenyl)-4-methylpiperazine-1-carboxamide (Compound 7).—To a solution of triphosgene (20 mg,

0.067 mmol, 1.0 equiv) in DCM (2 mL), DIPEA (8.7 mg, 0.067 mmol, 1.0 equiv) was added at 0 °C, and the mixture then was stirred at 25 °C for 5 min. **S3** (89 mg, 0.20 mmol, 3.0 equiv) was added to the reaction mixture and stirred at 25 °C for 30 min. 1-methylpiperazine (20 mg, 0.20 mmol, 3.0 equiv) was added to the reaction mixture and stirred for 2 h at 25 °C. LC-MS showed that one main peak was detected with the desired MS. The reaction

mixture was poured into water (15 mL) and the reaction was extracted with chloroform/isopropanol (v/v = 4:1, 3 × 50 mL). The reaction mixture was dried over Na₂SO₄, filtered, and concentrated under reduced pressure to give a residue. The residue was purified by preparative HPLC to give compound **7** (12 mg, 31% yield) as a white powder. ¹H NMR (500 MHz, DMSO-*d*₆) δ 10.60 (s, 1H), 9.22 (s, 1H), 8.19 (d, *J* = 2.2 Hz, 1H), 8.10 (dd, *J* = 8.5, 2.2 Hz, 1H), 7.99 (t, *J* = 1.8 Hz, 1H), 7.91 (t, *J* = 2.0 Hz, 1H), 7.73 (d, *J* = 8.6 Hz, 1H), 7.69 (t, *J* = 1.7 Hz, 1H), 4.27 (d, *J* = 14.3 Hz, 2H), 3.70 (s, 2H), 3.48 (d, *J* = 11.1 Hz, 4H), 3.21–3.12 (m, 4H), 3.08–2.91 (m, 6H), 2.85 (s, 3H), 2.41 (t, *J* = 12.3 Hz, 2H), 1.22 (t, *J* = 7.3 Hz, 3H). MS (ESI): calcd. for C₂₇H₃₅ClF₃N₆O₂ [M + H]⁺ 567.25, found 567.33.

3-Benzamido-5-chloro-N-(4-((4-ethylpiperazin-1-yl)-methyl)-3-(trifluoromethyl)phenyl)benzamide (Compound 8).—The

title compound was prepared according to the general procedure HATU-mediated amide formation pathway. White powder (18 mg, 39%). ¹H NMR (500 MHz, DMSO-*d*₆) δ 10.66 (s, 1H), 10.63 (s, 1H), 8.32 (t, *J* = 1.8 Hz, 1H), 8.18 (dt, *J* = 3.9, 2.0 Hz, 2H), 8.10 (dd, *J* = 8.5, 2.2 Hz, 1H), 8.04–7.96 (m, 2H), 7.79 (t, *J* = 1.7 Hz, 1H), 7.73 (d, *J* = 8.5 Hz, 1H), 7.66–7.59 (m, 1H), 7.58–7.52 (m, 2H), 3.68 (s, 2H), 3.45 (d, *J* = 12.0 Hz, 2H), 3.13 (q, *J* = 7.4 Hz, 2H), 3.03–2.87 (m, 4H), 2.41 (t, *J* = 12.1 Hz, 2H), 1.21 (t, *J* = 7.3 Hz, 3H). (ESI): calcd. for C₂₈H₂₉ClF₃N₄O₂⁺ [M + H]⁺ 545.19, found 545.53.

3-Chloro-N-(4-((4-ethylpiperazin-1-yl)methyl)-3-(trifluoromethyl)phenyl)-5-(3-(thiophen-2-yl)benzamido)-benzamide (Compound 9).—The title compound

was prepared according to the general procedure HATU-mediated amide formation pathway. White powder (15 mg, 23%). ¹H NMR (500 MHz, DMSO-*d*₆) δ 10.74 (s, 1H), 10.68 (s, 1H), 8.35 (t, *J* = 1.8 Hz, 1H), 8.24 (t, *J* = 1.8 Hz, 1H), 8.22 (q, *J* = 2.0 Hz, 2H), 8.13 (dd, *J* = 8.5, 2.2 Hz, 1H), 7.96–7.90 (m, 2H), 7.84 (t, *J* = 1.7 Hz, 1H), 7.76 (d, *J* = 8.5 Hz, 1H), 7.69–7.60 (m, 3H), 7.22 (dd, *J* = 5.1, 3.6 Hz, 1H), 3.71 (s, 2H), 3.49 (s, 2H), 3.16 (q, *J* = 7.6 Hz, 2H), 3.06–2.92 (m, 4H), 2.46–2.38 (m, 2H), 1.23 (t, *J* = 7.3 Hz, 3H). (ESI): calcd. for C₃₂H₃₁ClF₃N₄O₂S⁺ [M + H]⁺ 627.18, found 627.30.

N-(3-Chloro-5-((4-((4-ethylpiperazin-1-yl)methyl)-3-(trifluoromethyl)phenyl)carbamoyl)phenyl)pyrimidine-5-carboxamide (Compound 10).—The title compound was prepared according

to the general procedure HATU-mediated amide formation pathway. White powder (12 mg, 32%). ¹H NMR (500 MHz, DMSO-*d*₆) δ 10.96 (s, 1H), 10.67 (s, 1H), 9.40 (s, 1H), 9.30 (s, 2H), 8.26 (t, *J* = 1.8 Hz, 1H), 8.19 (d, *J* = 2.3 Hz, 1H), 8.15 (t, *J* = 1.9 Hz, 1H), 8.10 (dd, *J* = 8.5, 2.2 Hz, 1H), 7.86 (t, *J* = 1.7 Hz, 1H), 7.73 (d, *J* = 8.6 Hz, 1H), 3.69 (s, 2H), 3.46 (d, *J* = 12.0 Hz, 2H), 3.14 (q, *J* = 7.3 Hz, 2H), 3.02–2.91 (m, 4H), 2.43–2.35 (m, 2H), 1.21 (t, *J* = 7.3 Hz, 3H). MS (ESI): calcd. for C₂₆H₂₇ClF₃N₆O₂⁺ [M + H]⁺ 547.18, found 547.23.

2-Amino-N-(3-chloro-5-((4-((4-ethylpiperazin-1-yl)-methyl)-3-(trifluoromethyl)phenyl)carbamoyl)phenyl)-pyrimidine-5-carboxamide (Compound 11).—tert-

Butyl (tert-butoxycarbonyl)(5-((3-chloro-5-((4-((4-ethylpiperazin-1-yl)-methyl)-3-(trifluoromethyl)phenyl)carbamoyl)phenyl)-carbamoyl)pyrimidin-2-yl)carbamate

(di-Boc-**11**) was synthesized according to the general procedure HATU-mediated amide formation pathway. To a stirred solution of the above di-Boc-**11** in CH₂Cl₂ (2 mL) was added TFA (2 mL) at 0 °C. The reaction mixture was slowly warmed to ambient temperature and stirred for 1 h. Solvents and volatiles were removed in vacuo. The residue was purified by preparative HPLC to give the final compound **11** as a white solid (28 mg, 27% for 2 steps). ¹H NMR (500 MHz, DMSO-*d*₆) δ 10.65 (s, 1H), 10.39 (s, 1H), 8.84 (s, 2H), 8.25 (t, *J* = 1.8 Hz, 1H), 8.20 (d, *J* = 2.2 Hz, 1H), 8.16–8.08 (m, 2H), 7.79 (t, *J* = 1.8 Hz, 1H), 7.74 (d, *J* = 8.5 Hz, 1H), 7.44 (s, 2H), 3.70 (s, 2H), 3.47 (d, *J* = 12.0 Hz, 2H), 3.16 (q, *J* = 7.5 Hz, 2H), 2.98 (dd, *J* = 25.0, 11.4 Hz, 4H), 2.41 (dd, *J* = 12.2 Hz, 2H), 1.22 (t, *J* = 7.3 Hz, 3H). MS (ESI): calcd. for C₂₆H₂₈ClF₃N₇O₂⁺ [M + H]⁺ 562.19, found 562.23.

N-(3-Chloro-5-((4-((4-ethylpiperazin-1-yl)methyl)-3-(trifluoromethyl)phenyl)carbamoyl)phenyl)-5-cyanonicotinamide (Compound 12).—The title compound

was prepared according to the general procedure acid chloride pathway. White solid (20 mg, 31%). ¹H NMR (500 MHz, DMSO-*d*₆) δ 10.96 (s, 1H), 10.69 (s, 1H), 9.36 (d, *J* = 2.1 Hz, 1H), 9.26 (d, *J* = 2.0 Hz, 1H), 8.85 (t, *J* = 2.1 Hz, 1H), 8.28 (t, *J* = 1.8 Hz, 1H), 8.20 (d, *J* = 2.2 Hz, 1H), 8.18 (t, *J* = 1.9 Hz, 1H), 8.11 (dd, *J* = 8.4, 2.2 Hz, 1H), 7.88 (t, *J* = 1.7 Hz, 1H), 7.75 (d, *J* = 8.5 Hz, 1H), 3.71 (s, 2H), 3.48 (d, *J* = 11.9 Hz, 2H), 3.16 (q, *J* = 7.3 Hz, 2H), 3.00 (s, 2H), 2.95 (d, *J* = 13.5 Hz, 2H), 2.41 (t, *J* = 12.1 Hz, 2H), 1.22 (t, *J* = 7.3 Hz, 3H). MS (ESI): calcd. for C₂₈H₂₇ClF₃N₆O₂⁺ [M + H]⁺ 571.18, found 571.24.

N-(3-Chloro-5-((4-((4-ethylpiperazin-1-yl)methyl)-3-(trifluoromethyl)phenyl)carbamoyl)phenyl)-5-(furan-2-yl)-nicotinamide (Compound 13).—The title compound

was prepared according to the general procedure HATU-mediated amide formation pathway. Pale brown solid (35 mg, 57%). ¹H NMR (500 MHz, DMSO-*d*₆) δ 11.01 (s, 1H), 10.79 (s, 1H), 9.25 (d, *J* = 2.1 Hz, 1H), 9.12 (d, *J* = 2.1 Hz, 1H), 8.68 (t, *J* = 2.1 Hz, 1H), 8.41 (t, *J* = 1.7 Hz, 1H), 8.30 (q, *J* = 1.8 Hz, 2H), 8.21 (dd, *J* = 8.5, 2.2 Hz, 1H), 8.01 (dd, *J* = 1.8, 0.7 Hz, 1H), 7.94 (t, *J* = 1.7 Hz, 1H), 7.84 (d, *J* = 8.6 Hz, 1H), 7.36 (dd, *J* = 3.5, 0.8 Hz, 1H), 6.81 (dd, *J* = 3.5, 1.8 Hz, 1H), 3.81 (s, 2H), 3.57 (d, *J* = 11.9 Hz, 2H), 3.24 (q, *J* = 7.3 Hz, 2H), 3.16–2.99 (m, 4H), 2.54 (d, *J* = 12.5 Hz, 2H), 1.31 (t, *J* = 7.3 Hz, 3H). MS (ESI): calcd. for C₃₁H₃₀ClF₃N₅O₃⁺ [M + H]⁺ 612.20, found 612.24.

N-(3-Chloro-5-((4-((4-ethylpiperazin-1-yl)methyl)-3-(trifluoromethyl)phenyl)carbamoyl)phenyl)-5-phenylnicotinamide (Compound 14).—The title compound was prepared according to the general procedure

acid chloride pathway. White solid (19 mg, 27%). ¹H NMR (500 MHz, DMSO-*d*₆) δ 10.87 (s, 1H), 10.68 (s, 1H), 9.13 (dd, *J* = 7.1, 2.2 Hz, 2H), 8.62 (t, *J* = 2.2 Hz, 1H), 8.33 (t, *J* = 1.7 Hz, 1H), 8.24–8.18 (m, 2H), 8.12 (dd, *J* = 8.5, 2.2 Hz, 1H), 7.90–7.84 (m, 3H), 7.75 (d, *J* = 8.5 Hz, 1H), 7.62–7.55 (m, 2H), 7.54–7.47 (m, 1H), 3.71 (s, 2H), 3.47 (d, *J* = 12.0 Hz, 2H), 3.20–3.06 (m, 2H), 2.98 (dd, *J* = 27.0, 12.0 Hz, 4H), 2.43–2.33 (m, 2H), 1.22 (t, *J* = 7.3 Hz, 3H). MS (ESI): calcd. for C₃₃H₃₂ClF₃N₅O₂⁺ [M + H]⁺ 622.22, found 622.25.

N-(3-Chloro-5-((4-((4-ethylpiperazin-1-yl)methyl)-3-(trifluoromethyl)phenyl)carbamoyl)phenyl)-5-(thiazol-5-yl)-nicotinamide (Compound 15).—The title compound was prepared according to the general procedure acid chloride pathway. White solid (21 mg, 37%). ¹H NMR (500 MHz, DMSO-*d*₆) δ 10.90 (s, 1H), 10.69 (s, 1H), 9.26 (s, 1H), 9.18 (d, *J* = 2.2 Hz, 1H), 9.09 (d, *J* = 2.0 Hz, 1H), 8.62–8.55 (m, 2H), 8.31 (d, *J* = 1.8 Hz, 1H), 8.20 (t, *J* = 1.7 Hz, 2H), 8.15–8.09 (m, 1H), 7.87 (t, *J* = 1.8 Hz, 1H), 7.75 (d, *J* = 8.5 Hz, 1H), 3.71 (s, 2H), 3.48 (d, *J* = 12.0 Hz, 2H), 3.16 (q, *J* = 7.3 Hz, 2H), 3.01 (s, 2H), 2.95 (d, *J* = 13.4 Hz, 2H), 2.40 (t, *J* = 12.0 Hz, 2H), 1.22 (t, *J* = 7.3 Hz, 3H). ¹³C NMR (125 MHz, DMSO-*d*₆) δ 164.67, 164.51, 158.68, 158.41, 149.12, 147.89, 140.88, 140.77, 139.12, 134.23, 133.30, 132.34, 132.16, 131.35, 130.97, 129.95, 129.33, 128.19, 126.47, 125.76, 116.05, 115.91, 111.17, 57.01, 51.14, 51.07, 49.95, 9.47. MS (ESI): calcd. for C₃₀H₂₉ClF₃N₆O₂S⁺ [M + H]⁺ 629.17, found 629.30.

N-(3-Chloro-5-((4-((4-ethylpiperazin-1-yl)methyl)-3-(trifluoromethyl)phenyl)carbamoyl)phenyl)-5-(4-cyanophenyl)nicotinamide (Compound 16).—The title compound was prepared according to the general procedure HATU-mediated amide formation pathway. White solid (27 mg, 46%). ¹H NMR (500 MHz, DMSO-*d*₆) δ 10.88 (s, 1H), 10.68 (s, 1H), 9.21 (d, *J* = 2.3 Hz, 1H), 9.19 (s, 1H), 8.70 (t, *J* = 2.1 Hz, 1H), 8.31 (t, *J* = 1.7 Hz, 1H), 8.23–8.18 (m, 2H), 8.15–8.03 (m, 5H), 7.87 (t, *J* = 1.7 Hz, 1H), 7.75 (d, *J* = 8.5 Hz, 1H), 3.70 (s, 2H), 3.47 (d, *J* = 12.0 Hz, 2H), 3.19–3.13 (m, 2H), 2.97 (dd, *J* = 28.4, 12.4 Hz, 4H), 2.40 (d, *J* = 12.1 Hz, 2H), 1.22 (t, *J* = 7.3 Hz, 3H). MS (ESI): calcd. for C₃₄H₃₁ClF₃N₆O₂⁺ [M + H]⁺ 647.21, found 647.40.

3-Chloro-N-(4-((4-ethylpiperazin-1-yl)methyl)-3-(trifluoromethyl)phenyl)-5-((5-(thiophen-2-yl)pyridin-3-yl)-amino)benzamide (Compound 17).—To a solution of 3-bromo-5-(thiophen-2-yl) pyridine (49 mg, 0.2 mmol) and **S3** (60 mg, 0.14 mmol) in 2-MeTHF (3 mL), tribasic potassium phosphate (87 mg, 0.41 mmol), *t*-BuBrettPhos Pd G3 (23 mg, 0.03 mmol), and *t*-BuBrettPhos (13 mg, 0.03 mmol) were added at room temperature. The vial was evacuated and purged with nitrogen (3×). The reaction was warmed to 80 °C with stirring and maintained at this temperature overnight. Upon cooling to RT, the mixture was diluted with EtOAc and sat. aq. NH₄Cl. The biphasic mixture was transferred to a separatory funnel where the phases were mixed and then separated. The aqueous phase was extracted with additional EtOAc. The combined organic phases were washed with brine, dried over anhydrous Na₂SO₄, and filtered, and the collected filtrate was concentrated to dryness in vacuo. The crude residue was subjected to purification by flash chromatography over silica gel (0–8% MeOH/DCM) to afford the crude compound. Then the crude compound was purified by preparative HPLC to give compound **17** (19 mg, 23.0% yield) as a white powder. ¹H NMR (500 MHz, DMSO-*d*₆) δ 10.59 (s, 1H), 9.03 (s, 1H), 8.54 (d, *J* = 2.0 Hz, 1H), 8.42 (d, *J* = 2.5 Hz, 1H), 8.19 (d, *J* = 2.2 Hz, 1H), 8.09 (dd, *J* = 8.5, 2.2 Hz, 1H), 7.80 (t, *J* = 2.2 Hz, 1H), 7.73 (d, *J* = 8.5 Hz, 1H), 7.70–7.66 (m, 2H), 7.65 (t, *J* = 1.8 Hz, 1H), 7.56 (t, *J* = 1.6 Hz, 1H), 7.35 (t, *J* = 2.0 Hz, 1H), 7.21 (dd, *J* = 5.1, 3.6 Hz, 1H), 3.70 (s, 2H), 3.47 (d, *J* = 12.0 Hz, 2H), 3.15 (q, *J* = 7.3 Hz, 2H), 3.00 (s, 4H), 2.43–2.35 (m, 2H), 1.22 (t, *J* = 7.3 Hz, 3H). MS (ESI): calcd. for C₃₀H₃₀ClF₃N₆OS⁺ [M + H]⁺ 600.18, found 600.20.

3-Chloro-N-(4-((4-ethylpiperazin-1-yl)methyl)-3-(trifluoromethyl)phenyl)-5-(((5-(thiophen-2-yl)pyridin-3-yl)-methyl)amino)benzamide (Compound 18).—To a solution of **S3** (22 mg, 0.05 mmol, 1.0 equiv) and 5-(thiophen-2-yl) nicotinaldehyde (14 mg, 0.075 mmol, 1.5 equiv) in AcOH (1 mL), NaBH₃CN (9.3 mg, 0.15 mmol, 3.0 equiv) was added at 0 °C. The mixture then was stirred at 25 °C for 2 h. LC–MS showed that **S3** was consumed completely and one main peak with desired MS was detected. The reaction mixture was poured into saturated aqueous sodium bicarbonate (20 mL) and the reaction was extracted with chloroform/isopropanol (v/v = 4:1, 3 × 50 mL). The reaction mixture was then dried over Na₂SO₄, filtered, and concentrated under reduced pressure to give a residue. The residue was purified by preparative HPLC to give compound **18** (15 mg, 49% yield) as a white powder. ¹H NMR (500 MHz, DMSO-*d*₆) δ 10.46 (s, 1H), 8.87 (d, *J* = 2.2 Hz, 1H), 8.55 (d, *J* = 1.9 Hz, 1H), 8.18 (d, *J* = 2.2 Hz, 1H), 8.12 (t, *J* = 2.2 Hz, 1H), 8.06 (dd, *J* = 8.5, 2.2 Hz, 1H), 7.73–7.63 (m, 3H), 7.24–7.17 (m, 2H), 7.15 (t, *J* = 1.9 Hz, 1H), 6.89 (t, *J* = 2.0 Hz, 1H), 4.48 (s, 2H), 3.69 (s, 2H), 3.47 (d, *J* = 12.0 Hz, 2H), 3.15 (q, *J* = 7.3 Hz, 2H), 3.05–2.88 (m, 4H), 2.44–2.35 (m, 2H), 1.21 (t, *J* = 7.3 Hz, 3H). MS (ESI): calcd. for C₃₁H₃₂ClF₃N₅OS⁺ [M + H]⁺ 614.20, found 614.24.

N-(3-Chloro-5-(4-((4-ethylpiperazin-1-yl)methyl)-3-(trifluoromethyl)benzamido)phenyl)-5-(thiophen-2-yl)-nicotinamide (Compound 19).—Step 1: To

a solution of 3-chloro-5-nitroaniline (150 mg, 0.87 mmol) and **S4** (302 mg, 0.96 mmol) in DCM (8 mL) was added HATU (661 mg, 1.74 mmol) and DIPEA (561 mg, 4.35 mmol, 0.77 mL) at 0 °C. The mixture was stirred at 25 °C for 4 h. LC–MS showed 3-chloro-5-nitroaniline was consumed completely and one main peak with desired MS was detected. The reaction mixture was poured into water (15 mL) and the reaction was extracted with chloroform/isopropanol (v/v = 4:1, 3 × 60 mL). The organic phase was dried over Na₂SO₄ and filtered under reduced pressure. The crude residue was subjected to purification by flash chromatography over silica gel (0–5% MeOH/DCM) to afford the nitro compound.

Step 2: To a solution of the above compound (200 mg, 0.43 mmol) in EtOH (4 mL) and H₂O (2.0 mL) were added NH₄Cl (67.5 mg, 1.27 mmol) and Fe (119 mg, 2.12 mmol) at 25 °C. The mixture was stirred at 80 °C for 2 h. The reaction mixture was filtered and concentrated under reduced pressure to remove EtOH. The reaction mixture was poured into water (15 mL) and extracted with chloroform/isopropanol (v/v = 4:1, 3 × 60 mL). The combined organic phase was washed with saturated brine (30 mL), dried over Na₂SO₄, filtered, and concentrated in vacuum to give **S5** as a white solid.

Step 3: To a solution of **S5** (50 mg, 0.11 mmol) and 5-(thiophen-2-yl)nicotinic acid (35 mg, 0.17 mmol) in DMF (2 mL), 1-[bis(dimethylamino)methylene]-1H-1,2,3-triazolo[4,5-*b*]pyridinium 3-oxide hexafluorophosphate (HATU) (82 mg, 0.34 mmol) and N,N-diisopropylethylamine (DIPEA) (73 mg, 0.57 mmol) were added at 0 °C. This mixture then was stirred at 25 °C for 12 h. LC–MS showed that **S5** was consumed completely and one main peak with the desired MS was detected. The reaction mixture was poured into water (15 mL) and was extracted with ethyl acetate (3 × 50 mL). The reaction mixture was then dried over Na₂SO₄, filtered, and concentrated under reduced pressure to give a residue.

The residue was purified by preparative HPLC to give the final compound **19** (28 mg, 39%) as white powder. ¹H NMR (500 MHz, DMSO-*d*₆) δ 10.68 (s, 1H), 10.62 (s, 1H), 9.05 (d, *J* = 2.3 Hz, 1H), 8.94 (d, *J* = 2.1 Hz, 1H), 8.43 (t, *J* = 2.2 Hz, 1H), 8.28 (t, *J* = 1.9 Hz, 1H), 8.25 (d, *J* = 1.9 Hz, 1H), 8.20 (dd, *J* = 8.1, 1.9 Hz, 1H), 7.88 (d, *J* = 8.1 Hz, 1H), 7.72 (dd, *J* = 3.7, 1.2 Hz, 1H), 7.67 (dd, *J* = 5.0, 1.1 Hz, 1H), 7.64 (t, *J* = 1.9 Hz, 1H), 7.60 (t, *J* = 2.0 Hz, 1H), 7.19 (dd, *J* = 5.1, 3.6 Hz, 1H), 3.74 (s, 2H), 3.41 (d, *J* = 12.0 Hz, 2H), 3.14–3.05 (m, 2H), 2.96 (d, *J* = 11.0 Hz, 2H), 2.88 (d, *J* = 12.8 Hz, 2H), 2.41–2.32 (m, 2H), 1.15 (t, *J* = 7.2 Hz, 3H). ¹³C NMR (126 MHz, DMSO-*d*₆) δ 164.68, 164.52, 158.69, 158.42, 149.13, 147.90, 140.89, 140.78, 139.12, 134.23, 133.31, 132.35, 132.17, 131.36, 130.98, 129.96, 129.33, 128.19, 126.47, 125.81, 123.47, 116.06, 115.92, 111.18, 57.01, 51.14, 51.07, 49.95, 9.47. MS (ESI): calcd. for C₃₁H₃₀ClF₃N₅O₂S⁺ [M + H]⁺ 628.18, found 628.20.

5-Chloro-N1-(4-((4-ethylpiperazin-1-yl)methyl)-3-(trifluoromethyl)phenyl)-N3-(5-(thiophen-2-yl)pyridin-3-yl)-isophthalamide (Compound 20).—Step 1: To a

solution of 3-chloro-5-(methoxycarbonyl)benzoic acid (201 mg, 0.94 mmol) and **S6** (245 mg, 0.85 mmol) in DCM (8 mL) were added HATU (648 mg, 1.71 mmol) and DIPEA (550 mg, 4.26 mmol, 0.75 mL) at 0 °C. The mixture was stirred at 25 °C for 4 h. LC-MS showed **S6** was consumed completely and one main peak with desired MS was detected. The reaction mixture was poured into water (15 mL) and the reaction was extracted with chloroform/isopropanol (v/v = 4:1, 3 × 60 mL). The organic phase was dried over Na₂SO₄ and filtered under reduced pressure. The crude residue was subjected to purification by flash chromatography over silica gel (0–5% MeOH/DCM) to afford the methyl ester compound.

Step 2: To a solution of the above compound (200 mg, 0.41 mmol) in THF (3 mL) and MeOH (1 mL) was added NaOH (21.5 mg, 0.54 mmol, dissolved in 1 mL H₂O) in one portion at 0 °C. The mixture was stirred at room temperature for 2 h. LC-MS showed ester was consumed completely and one main peak with desired MS was detected. The reaction mixture was concentrated in vacuo. The residue was dissolved in H₂O (3 mL) and then acidified to pH 5.0 with 1.0 N aq. HCl at 0 °C. The precipitate was collected and dried under vacuum to provide **S7** as pale brown solid.

Step 3: To a solution of **S7** (52 mg, 0.11 mmol) and 5-(thiophen-2-yl)pyridin-3-amine (15 mg, 0.085 mmol) in DMF (2 mL), 1-[bis(dimethylamino)methylene]-1H-1,2,3-triazolo-[4,5-*b*]pyridinium 3-oxide hexafluorophosphate (HATU) (65 mg, 0.17 mmol) and N,N-diisopropylethylamine (DIPEA) (58 mg, 0.43 mmol) were added at 0 °C. This mixture then was stirred at 25 °C for 12 h. LC-MS showed that 5-(thiophen-2-yl)pyridin-3-amine was consumed completely and one main peak with the desired MS was detected. The reaction mixture was poured into water (15 mL) and was extracted with ethyl acetate (3 × 50 mL). The reaction mixture was then dried over Na₂SO₄, filtered, and concentrated under reduced pressure to give a residue. The residue was purified by preparative HPLC to give the final compound **20** (19 mg, 36%) as white powder. ¹H NMR (500 MHz, DMSO-*d*₆) δ 10.60 (d, *J* = 3.7 Hz, 1H), 9.02 (s, 1H), 8.54 (d, *J* = 2.2 Hz, 1H), 8.41 (d, *J* = 2.7 Hz, 1H), 8.19 (d, *J* = 2.2 Hz, 1H), 8.09 (dd, *J* = 8.5, 2.2 Hz, 1H), 7.79 (d, *J* = 2.6 Hz, 1H), 7.73 (d, *J* = 8.6 Hz, 1H), 7.68 (ddt, *J* = 6.9, 3.6, 1.8 Hz, 2H), 7.65 (q, *J* = 1.8 Hz, 1H), 7.56 (q, *J* = 1.9 Hz, 1H), 7.37–7.32 (m, 1H), 7.21 (ddd, *J* = 5.0, 3.7, 0.9 Hz, 1H), 3.70 (s, 2H), 3.47 (d, *J* = 12.0 Hz,

2H), 3.19–3.10 (m, 2H), 3.05–2.89 (m, 4H), 2.41 (d, $J = 12.5$ Hz, 2H), 1.22 (t, $J = 7.3$ Hz, 3H). MS (ESI): calcd. for $C_{31}H_{30}ClF_3N_5O_2S^+$ $[M + H]^+$ 628.18, found 628.30.

N-(3-Chloro-5-((3-(trifluoromethyl)phenyl)carbamoyl)-phenyl)-5-(thiophen-2-yl)nicotinamide (Compound 21).—The title compound was prepared according to the general procedure acid chloride pathway. White powder (23 mg, 31%). 1H NMR (500 MHz, DMSO- d_6) δ 10.89 (s, 1H), 10.69 (s, 1H), 9.13 (d, $J = 2.2$ Hz, 1H), 9.04 (d, $J = 2.0$ Hz, 1H), 8.54 (t, $J = 2.2$ Hz, 1H), 8.28 (t, $J = 1.8$ Hz, 1H), 8.23 (dt, $J = 5.8, 1.9$ Hz, 2H), 8.08 (dd, $J = 8.1, 2.0$ Hz, 1H), 7.87 (t, $J = 1.8$ Hz, 1H), 7.80 (dd, $J = 3.7, 1.2$ Hz, 1H), 7.75 (dd, $J = 5.1, 1.1$ Hz, 1H), 7.64 (t, $J = 8.0$ Hz, 1H), 7.50 (d, $J = 7.8$ Hz, 1H), 7.27 (dd, $J = 5.0, 3.6$ Hz, 1H). MS (ESI): calcd. for $C_{24}H_{16}ClF_3N_3O_2S^+$ $[M + H]^+$ 502.06, found 502.12.

N-(3-Chloro-5-((4-((4-ethylpiperazin-1-yl)methyl)phenyl)-carbamoyl)phenyl)-5-(thiophen-2-yl)nicotinamide (Compound 22).—The title compound was prepared according to the general procedure HATU-mediated amide formation pathway. White powder (15 mg, 34%). 1H NMR (500 MHz, DMSO- d_6) δ 10.94 (s, 1H), 10.57 (s, 1H), 9.13 (d, $J = 2.2$ Hz, 1H), 9.05 (d, $J = 2.0$ Hz, 1H), 8.57 (t, $J = 2.2$ Hz, 1H), 8.31 (t, $J = 1.7$ Hz, 1H), 8.23 (t, $J = 2.0$ Hz, 1H), 7.89–7.83 (m, 3H), 7.83–7.80 (m, 1H), 7.76 (dd, $J = 5.2, 1.1$ Hz, 1H), 7.64–7.50 (m, 2H), 7.27 (dd, $J = 5.1, 3.6$ Hz, 1H), 4.39–3.82 (m, 6H), 3.79–3.12 (m, 6H), 1.24 (t, $J = 6.7$ Hz, 3H). MS (ESI): calcd. for $C_{30}H_{31}ClN_5O_2S^+$ $[M + H]^+$ 560.19, found 560.18.

N-(3-Chloro-5-((2-morpholinopyridin-4-yl)carbamoyl)-phenyl)-5-(thiophen-2-yl)nicotinamide (Compound 23).—The title compound was prepared according to the general procedure acid chloride pathway. White powder (21 mg, 27%). 1H NMR (500 MHz, DMSO- d_6) δ 11.01 (s, 1H), 10.91 (s, 1H), 9.14 (d, $J = 2.2$ Hz, 1H), 9.04 (d, $J = 2.0$ Hz, 1H), 8.53 (t, $J = 2.2$ Hz, 1H), 8.33 (t, $J = 1.8$ Hz, 1H), 8.21 (t, $J = 1.9$ Hz, 1H), 8.08 (d, $J = 6.6$ Hz, 1H), 7.85 (t, $J = 1.7$ Hz, 1H), 7.80 (dd, $J = 3.6, 1.2$ Hz, 1H), 7.76 (dd, $J = 5.1, 1.1$ Hz, 1H), 7.66 (s, 1H), 7.34 (d, $J = 6.7$ Hz, 1H), 7.27 (dd, $J = 5.1, 3.6$ Hz, 1H), 3.81–3.76 (m, 4H), 3.53 (t, $J = 4.9$ Hz, 4H). MS (ESI): calcd. for $C_{26}H_{23}ClN_5O_3S^+$ $[M + H]^+$ 520.12, found 520.27.

N-(5-((4-((4-Ethylpiperazin-1-yl)methyl)-3-(trifluoromethyl)phenyl)carbamoyl)-2-fluorophenyl)-5-(thio-phen-2-yl)nicotinamide (Compound 24).—The title compound was prepared according to the general procedure acid chloride pathway. 1H NMR (500 MHz, DMSO- d_6) δ 10.75 (s, 1H), 10.68 (s, 1H), 9.19 (d, $J = 2.2$ Hz, 1H), 9.10 (d, $J = 2.1$ Hz, 1H), 8.60 (t, $J = 2.1$ Hz, 1H), 8.36 (dd, $J = 7.3, 2.3$ Hz, 1H), 8.26 (d, $J = 2.3$ Hz, 1H), 8.15 (dd, $J = 8.5, 2.3$ Hz, 1H), 8.02 (ddd, $J = 8.7, 4.6, 2.3$ Hz, 1H), 7.87–7.76 (m, 3H), 7.60 (dd, $J = 10.1, 8.6$ Hz, 1H), 7.31 (dd, $J = 4.9, 3.5$ Hz, 1H), 3.75 (s, 2H), 3.60–3.43 (m, 2H), 3.20 (q, $J = 7.3$ Hz, 2H), 3.03 (dd, $J = 26.6, 9.2$ Hz, 4H), 2.46 (t, $J = 12.3$ Hz, 2H), 1.27 (t, $J = 7.4$ Hz, 3H). MS (ESI): calcd. for $C_{31}H_{30}F_4N_5O_2S^+$ $[M + H]^+$ 612.21, found 612.18.

N-(5-((4-((4-Ethylpiperazin-1-yl)methyl)-3-(trifluoromethyl)phenyl)carbamoyl)-2-methoxyphenyl)-5-(thiophen-2-yl)nicotinamide (Compound 25).—The title compound was prepared according to the general procedure acid chloride pathway. 1H NMR (500 MHz, DMSO- d_6) δ 10.51 (s, 1H), 10.20 (s, 1H), 9.17 (d, $J = 2.3$ Hz, 1H), 9.08 (d, J

= 2.1 Hz, 1H), 8.59 (t, J = 2.2 Hz, 1H), 8.39 (d, J = 2.3 Hz, 1H), 8.27 (d, J = 2.3 Hz, 1H), 8.17 (d, J = 8.6 Hz, 1H), 8.01 (dd, J = 8.6, 2.3 Hz, 1H), 7.84 (d, J = 3.6 Hz, 1H), 7.78 (dd, J = 10.0, 6.7 Hz, 2H), 7.35 (d, J = 8.8 Hz, 1H), 7.31 (dd, J = 5.0, 3.6 Hz, 1H), 4.00 (s, 3H), 3.75 (s, 2H), 3.52–3.44 (m, 2H), 3.20 (q, J = 7.3 Hz, 2H), 3.12–2.94 (m, 4H), 2.44 (dd, J = 16.7, 7.1 Hz, 2H), 1.27 (t, J = 7.3 Hz, 3H). MS (ESI): calcd. for $C_{32}H_{33}F_3N_5O_3S^+$ [M + H]⁺ 624.23, found 624.11.

N-(3-((4-((4-Ethylpiperazin-1-yl)methyl)-3-(trifluoromethyl)phenyl)carbamoyl)-4-fluorophenyl)-5-(thiophen-2-yl)nicotinamide (Compound 26).—The title

compound was prepared according to the general procedure acid chloride pathway. White powder (45 mg, 39%). ¹H NMR (500 MHz, DMSO-*d*₆) δ 10.81 (s, 1H), 10.78 (s, 1H), 9.12 (d, J = 2.3 Hz, 1H), 9.03 (d, J = 2.1 Hz, 1H), 8.53 (t, J = 2.2 Hz, 1H), 8.19 (d, J = 2.3 Hz, 1H), 8.14 (dd, J = 6.3, 2.7 Hz, 1H), 8.05–7.94 (m, 2H), 7.79 (dd, J = 3.6, 1.2 Hz, 1H), 7.77–7.71 (m, 2H), 7.44 (t, J = 9.3 Hz, 1H), 7.26 (dd, J = 5.1, 3.6 Hz, 1H), 3.73 (s, 2H), 3.48 (d, J = 11.8 Hz, 2H), 3.16 (q, J = 7.3 Hz, 2H), 3.05–2.94 (m, 4H), 2.50–2.33 (m, 2H), 1.22 (t, J = 7.3 Hz, 3H). MS (ESI): calcd. for $C_{31}H_{30}F_4N_5O_2S^+$ [M + H]⁺ 612.21, found 612.24.

N-(5-((4-((4-Ethylpiperazin-1-yl)methyl)-3-(trifluoromethyl)phenyl)carbamoyl)-4-fluoro-2-methylphenyl)-5-(thiophen-2-yl)nicotinamide (Compound 27).—The

title compound was prepared according to the general procedure acid chloride pathway. ¹H NMR (500 MHz, DMSO-*d*₆) δ 10.76 (s, 1H), 10.43 (s, 1H), 9.17 (d, J = 2.3 Hz, 1H), 9.09 (d, J = 2.1 Hz, 1H), 8.58 (t, J = 2.2 Hz, 1H), 8.21 (d, J = 2.2 Hz, 1H), 8.05 (dd, J = 8.5, 2.2 Hz, 1H), 7.83 (dd, J = 3.6, 1.2 Hz, 1H), 7.80–7.73 (m, 3H), 7.42 (d, J = 10.9 Hz, 1H), 7.33–7.30 (m, 1H), 3.75 (s, 2H), 3.59 (s, 2H), 3.20 (p, J = 6.8 Hz, 2H), 3.08–2.93 (m, 4H), 2.47 (d, J = 17.6 Hz, 2H), 2.40 (s, 3H), 1.27 (t, J = 7.3 Hz, 3H). MS (ESI): calcd. for $C_{32}H_{32}F_4N_5O_2S^+$ [M + H]⁺ 626.22, found 626.16.

3-Amino-N-(4-((4-ethylpiperazin-1-yl)methyl)-3-(trifluoromethyl)phenyl)-5-methylbenzamide (Compound 28).—The title compound was prepared according

to the general procedure acid chloride pathway. White powder (55 mg, 29%). ¹H NMR (500 MHz, DMSO-*d*₆) δ 10.68 (s, 1H), 10.58 (s, 1H), 9.12 (d, J = 2.3 Hz, 1H), 9.04 (d, J = 2.0 Hz, 1H), 8.53 (t, J = 2.2 Hz, 1H), 8.22 (d, J = 2.2 Hz, 1H), 8.18 (d, J = 1.9 Hz, 1H), 8.13 (dd, J = 8.5, 2.2 Hz, 1H), 7.86 (d, J = 2.0 Hz, 1H), 7.80 (dd, J = 3.7, 1.2 Hz, 1H), 7.76–7.71 (m, 2H), 7.60 (s, 1H), 7.26 (dd, J = 5.1, 3.6 Hz, 1H), 3.70 (s, 2H), 3.48 (d, J = 12.0 Hz, 2H), 3.16 (q, J = 7.3 Hz, 2H), 3.04–2.91 (m, 4H), 2.45 (s, 3H), 2.40 (t, J = 11.9 Hz, 2H), 1.22 (t, J = 7.3 Hz, 3H). MS (ESI): calcd. for $C_{32}H_{33}F_3N_5O_2S^+$ [M + H]⁺ 608.23, found 608.29.

N-(4-((4-((4-Ethylpiperazin-1-yl)methyl)-3-(trifluoromethyl)phenyl)carbamoyl)pyridin-2-yl)-5-(thiophen-2-yl)nicotinamide (Compound 29).—The title

compound was prepared according to the general procedure acid chloride pathway. ¹H NMR (500 MHz, DMSO-*d*₆) δ 11.54 (s, 1H), 10.94 (s, 1H), 9.16 (d, J = 2.3 Hz, 1H), 9.13–9.06 (m, 1H), 8.75 (t, J = 1.1 Hz, 1H), 8.70 (dd, J = 3.8, 1.5 Hz, 2H), 8.28 (d, J = 2.2 Hz, 1H), 8.16 (dd, J = 8.5, 2.2 Hz, 1H), 7.86 (dd, J = 3.7, 1.2 Hz, 1H), 7.82 (d, J = 8.6 Hz, 1H), 7.79 (dd, J = 5.1, 1.2 Hz, 1H), 7.76 (dd, J = 5.1, 1.6 Hz, 1H), 7.34–7.28 (m, 1H), 3.77 (s, 2H),

3.62–3.42 (m, 2H), 3.21 (q, $J = 7.3$ Hz, 2H), 3.10–2.98 (m, 4H), 2.51–2.42 (m, 2H), 1.27 (t, $J = 7.3$ Hz, 3H). MS (ESI): calcd. for $C_{30}H_{30}F_3N_6O_2S^+$ $[M + H]^+$ 595.21, found 595.11.

N-(4-((4-Ethylpiperazin-1-yl)methyl)-3-(trifluoromethyl)-phenyl)-5-(5-(thiophen-2-yl)nicotinamido)nicotinamide (Compound 30).—The

title compound was prepared according to the general procedure acid chloride pathway. 1H NMR (500 MHz, DMSO- d_6) δ 11.04 (s, 1H), 10.89 (s, 1H), 9.22 (d, $J = 2.3$ Hz, 2H), 9.13 (d, $J = 2.1$ Hz, 1H), 9.02 (d, $J = 2.0$ Hz, 1H), 8.82 (t, $J = 2.2$ Hz, 1H), 8.62 (t, $J = 2.1$ Hz, 1H), 8.29 (d, $J = 2.2$ Hz, 1H), 8.18 (dd, $J = 8.5, 2.2$ Hz, 1H), 7.87 (dd, $J = 3.6, 1.2$ Hz, 1H), 7.85–7.79 (m, 2H), 7.33 (dd, $J = 5.1, 3.6$ Hz, 1H), 3.78 (s, 2H), 3.54 (d, $J = 12.0$ Hz, 2H), 3.23 (q, $J = 7.3$ Hz, 2H), 3.13–2.99 (m, 4H), 2.52–2.41 (m, 2H), 1.29 (t, $J = 7.3$ Hz, 3H). MS (ESI): calcd. for $C_{30}H_{30}F_3N_6O_2S^+$ $[M + H]^+$ 595.21, found 595.11.

N-(3-((4-((4-Ethylpiperazin-1-yl)methyl)-3-(trifluoromethyl)phenyl)carbamoyl)-5-fluorophenyl)-5-(thiophen-2-yl)nicotinamide (Compound 31).—The title

compound was prepared according to the general procedure acid chloride pathway. White powder (13 mg, 23%). 1H NMR (500 MHz, DMSO- d_6) δ 11.04 (s, 1H), 10.75 (s, 1H), 9.22 (d, $J = 2.3$ Hz, 1H), 9.13 (d, $J = 2.1$ Hz, 1H), 8.63 (t, $J = 2.2$ Hz, 1H), 8.32–8.25 (m, 2H), 8.20 (dd, $J = 8.4, 2.2$ Hz, 1H), 8.10 (dt, $J = 10.9, 2.2$ Hz, 1H), 7.89 (dd, $J = 3.6, 1.2$ Hz, 1H), 7.84 (dt, $J = 6.3, 1.5$ Hz, 2H), 7.72 (ddd, $J = 9.2, 2.4, 1.4$ Hz, 1H), 7.35 (dd, $J = 5.1, 3.6$ Hz, 1H), 3.81 (s, 2H), 3.57 (d, $J = 11.9$ Hz, 2H), 3.24 (q, $J = 7.3$ Hz, 2H), 3.14–3.00 (m, 4H), 2.52 (t, $J = 12.0$ Hz, 2H), 1.31 (t, $J = 7.3$ Hz, 3H). MS (ESI): calcd. for $C_{31}H_{30}F_4N_5O_2S^+$ $[M + H]^+$ 612.21, found 612.16.

N-(3-Bromo-5-((4-((4-ethylpiperazin-1-yl)methyl)-3-(trifluoromethyl)phenyl)carbamoyl)phenyl)-5-(thiophen-2-yl)nicotinamide (Compound 32).—The title compound was prepared

according to the general procedure acid chloride pathway. White powder (30 mg, 27%). 1H NMR (500 MHz, DMSO- d_6) δ 10.88 (s, 1H), 10.69 (s, 1H), 9.14 (d, $J = 2.3$ Hz, 1H), 9.04 (d, $J = 2.0$ Hz, 1H), 8.54 (t, $J = 2.2$ Hz, 1H), 8.36 (t, $J = 1.7$ Hz, 1H), 8.34 (t, $J = 1.9$ Hz, 1H), 8.20 (d, $J = 2.2$ Hz, 1H), 8.12 (dd, $J = 8.5, 2.2$ Hz, 1H), 7.99 (t, $J = 1.6$ Hz, 1H), 7.80 (dd, $J = 3.6, 1.2$ Hz, 1H), 7.78–7.73 (m, 2H), 7.27 (dd, $J = 5.1, 3.6$ Hz, 1H), 3.72 (s, 2H), 3.48 (d, $J = 11.9$ Hz, 2H), 3.16 (q, $J = 7.3$ Hz, 2H), 3.07–2.92 (m, 4H), 2.42 (t, $J = 12.3$ Hz, 2H), 1.22 (t, $J = 7.3$ Hz, 3H). MS (ESI): calcd. for $C_{31}H_{30}BrF_3N_5O_2S^+$ $[M + H]^+$ 672.13, found 672.21.

N-(3-((4-((4-Ethylpiperazin-1-yl)methyl)-3-(trifluoromethyl)phenyl)carbamoyl)-5-(trifluoromethyl)-phenyl)-5-(thiophen-2-yl)nicotinamide (Compound 33).—The

title compound was prepared according to the general procedure acid chloride pathway. White powder (11 mg, 20%). 1H NMR (500 MHz, CD $_3$ OD) δ 9.01 (t, $J = 2.2$ Hz, 2H), 8.59 (t, $J = 2.1$ Hz, 1H), 8.57 (t, $J = 1.8$ Hz, 1H), 8.36 (t, $J = 1.9$ Hz, 1H), 8.14 (d, $J = 2.2$ Hz, 1H), 8.04 (q, $J = 1.3$ Hz, 1H), 7.96 (dd, $J = 8.5, 2.3$ Hz, 1H), 7.77 (d, $J = 8.5$ Hz, 1H), 7.65 (dd, $J = 3.7, 1.2$ Hz, 1H), 7.57 (dd, $J = 5.1, 1.1$ Hz, 1H), 7.19 (dd, $J = 5.1, 3.7$ Hz, 1H), 3.68 (d, $J = 1.7$ Hz, 2H), 2.89–2.41 (m, 10H), 1.16 (t, $J = 7.2$ Hz, 3H). MS (ESI): calcd. for $C_{32}H_{30}F_3N_6O_2S^+$ $[M + H]^+$ 662.20, found 662.26.

METHODS

Culture Conditions.

P. falciparum strains, unless otherwise noted, were cultured in an adapted Trager and Jansen method.³⁹ Parasites were maintained at 4% hematocrit with A+ erythrocytes in RPMI 1640 medium supplemented with 26 mM sodium bicarbonate, 25 mM HEPES, 2% dextrose, 15 mg/L hypoxanthine, 25 mg/L gentamycin, and 0.5% AlbuMAX II (ThermoFisher, Waltham MA). *P. falciparum* strains Dd2 (MRA-156) and 3D7 (MRA-152) were incubated at 5% CO₂ and 37 °C while Cambodian clinical isolates, strains IPC 5188 (MRA-1239), strain IPC 5202 (MRA-1240), and IPC_6261 (MRA-1284) (BEI Resources, Manassas, VA) were incubated in 90% N₂, 5% O₂, and 5% CO₂ at 37 °C in a humidified modular incubator chamber (Billups Rothenberg, San Diego, CA, USA). Human HepG2 and MCF7 lines were maintained in Eagle's Minimal Essential Medium, supplemented with 1% antibiotic-antimycotic solution (Gemini Bio, West Sacramento, CA) and 10% fetal bovine serum in 5% CO₂ at 37 °C.

SYBR Green I Proliferation Assay.

This method was based on the previously described SYBR Green I-based assay.¹⁸ Briefly, intraerythrocytic *P. falciparum* cultures containing primarily ring stage (except for data reported in Table 1 where asynchronous cultures were used) were plated at 1% hematocrit and 1% parasitemia in 96-well flat-bottomed black plates with compound and incubated at 37 °C in 5% CO₂. As a control for no parasite growth, 5 μM chloroquine was used. The final DMSO concentration did not exceed 0.2%. After 72 h, plates were subjected to one freeze-thaw cycle at -80 °C and given 100 μL of lysis buffer (20 mM Tris-HCl, 5 mM EDTA, 0.8% Triton X-100, 0.08% saponin, and 1× SYBR Green I (Thermo Fisher, Waltham, MA)). Plates were incubated at RT, protected from light for 1 h, and read with a BioTek Synergy Neo2 multimode microplate reader (Winooski, VT). Fluorescence emission was detected at 485 nm excitation and 530 nm emission. Resulting values were normalized with full growth untreated controls and no growth chloroquine-treated controls. CDD Vault (Burlingame, CA) was used to calculate EC₅₀ values from at least three biological replicates.

Cytotoxicity Assay.

Human HepG2 hepatocytes (ATCC ID: HB-8065) or human MCF7 mammary gland adenocarcinoma (ATCC ID: HB-22) were seeded in clear flat-bottomed 384-well plates at a density of 2250 cells or 1000 cells per well, respectively. After 24 h of incubation in 5% CO₂ at 37 °C, the compound was applied in serial dilution, with DMSO concentrations not exceeding 0.25% and incubated for another 48 h. Negative control wells were treated for 10 min with 5% Triton X-100, and all wells received 10 μL CellTiter 96 Aqueous One Solution Reagent MTS 3-(4,5-dimethylthiazol-2-yl)-5-(3-carboxymethoxyphenyl)-2-(4-sulfophenyl)-2H-tetrazolium reagent (Promega, Madison, WI) and incubated at 37 °C for 3 h. The plate was then read at an absorbance of 490 nm with a BioTek Synergy Neo2 multimode microplate reader (Winooski, VT). Untreated cells and Triton X-100-treated cells were used to normalize the results, and EC₅₀ was calculated with CDD Vault (Burlingame, CA).

Rate of Killing Assay.

The assay used to evaluate the rate of killing was adapted from a previously described method.⁴⁰ Blood stage *P. falciparum* Dd2 cultures were plated at 4% hematocrit and 1% parasitemia into a 24-well plate, and wells were given $10 \times EC_{50}$ of compound **1** and incubated in standard culture conditions for 12, 24, or 48 h. At this point, the culture was washed once with fresh media, and parasites were monitored every 24 h thereafter up to 96 h. Per time point, Giemsa-stained thin blood smears were made, and culture samples were collected, washed in 0.5% BSA, and incubated with 60 μ M MitoTracker Deep Red FM (Thermo Fisher, Waltham, MA) and $1 \times SYBR$ Green I (Thermo Fisher, Waltham, MA) at 37 °C for 20 min. Samples were again washed in 0.5% BSA and resuspended in PBS. Samples were evaluated with a CytoFLEX S (Beckman Coulter, Brea, CA) flow cytometer, recording 100,000 events per sample. Data analysis was performed with FlowJo Version 10 software (Ashland, OR). The proportion of viable parasites was acquired by calculating the percent of SYBR Green I and MitoTracker double-positive cells. Gating was performed with the aid of four control samples: uninfected erythrocytes, untreated parasite culture, untreated culture stained only with MitoTracker, and DHA-treated culture.

Parasite Reduction Ratio (PRR) Assay.

This assay was based on the previously described Parasite Reduction Ratio (PRR) assay.²⁶ *P. falciparum* 3D7 blood-stage parasites were synchronized to mature schizonts with Percoll gradient or gelatin flotation.^{41,42} During reinvasion at 0–3 HPI, culture was shaken in a humidified chamber with 90% N₂, 5% O₂, and 5% CO₂ at 37 °C to prevent multiple infected RBCs, and this was followed by sorbitol synchronization.⁴³ Parasitemia was counted with Giemsa-stained thin blood smears, and the culture was diluted to 2% hematocrit and 0.5% parasitemia (1×10^6 parasites/mL). Culture is treated with $10 \times EC_{50}$ of the compound, and every 24 h the compound is washed out and media replenished until 120 h, which corresponds to two and a half asexual life cycles. At each time point, samples of the washed culture were serially diluted 1:3 in a round-bottom 96-well plate with uninfected RBCs. These plates were incubated for 21 days, with media change twice a week and hematocrit supplementation once a week. On day 21, plates were frozen, and parasite growth was assessed with a SYBR Green I-based assay as described above. The number of viable parasites per time point was calculated using the following formula: $\#viable\ parasites = X^n - 1$, where X is the serial dilution factor and n is the number of wells with parasite growth. Using GraphPad Prism 9 (San Diego, CA), the $\log((\# viable\ parasites) + 1)$ was graphed as a function of time, and the lag phase, parasite reduction rate (PRR), and 99.9% parasite clearance time (PCT) were determined from the curve.

Stage Specific Assay.

The stage-specific assay was performed as previously described.⁴⁴ Blood stage *P. falciparum* Dd2 parasites were synchronized to select early rings, 0–3 HPI. The first synchronization was with a magnetic MACS LD column (Cat. # 130–042–901, Miltenyi Biotec, Gaithersburg, MD), followed by 5% sorbitol treatment 3 h later.^{45,43} At 6 HPI, parasites were plated onto a 96-well plate at 1% hematocrit and 1% parasitemia, and $5 \times EC_{50}$ of compound **1** was added to the 6 HPI treatment wells. At intervals of 12 h, samples

were washed in PBS and fixed in 4% paraformaldehyde in PBS, supplemented with 0.075% glutaraldehyde. Giemsa-stained thin blood smears were also realized. At 54 HPI, samples were permeabilized with 0.25% Triton X-100 and treated with 50 $\mu\text{g}/\text{mL}$ RNase A before being stained with 500 nM YOYO-1 (Thermo Fisher, Waltham, MA). Finally, samples were washed in PBS and analyzed with a CytoFLEX S flow cytometer (Beckman Coulter, Brea, CA). Per sample, 100,000 events were collected, and uninfected RBCs served as a gating control. Analysis of results was performed with FlowJo software Version 10. For microscopy images, thin blood smears were fixed in methanol, stained in a 2% Giemsa solution for 12 min, and rinsed with distilled water. Images were acquired with a Nikon ECLIPSE Si microscope and a Nikon Plan Fluor 100 \times /1.3 oil immersion objective (Nikon Instruments, Melville, NY) and analyzed with the Nikon NIS-Elements Version 5.30.04 software.

Stage Specific SYBR Green I Proliferation Assay.

Determination of stage-specific EC_{50} was performed using a modified SYBR Green I proliferation assay, as described above. In this version, *P. falciparum* 3D7 was tightly synchronized to 0–3 HPI maintained at 37 °C in a humidified chamber with 90% N_2 , 5% O_2 , and 5% CO_2 . Every 10 h, 96-well black plates were given compound and parasites at 1% parasitemia, and 1% hematocrit. After 72 h, plates were frozen at –80 °C and read as described above.

Liver Stage Activity Assay.

Liver stage activity was evaluated as previously described.⁴⁶ Briefly, 3×10^3 of HepG2-A16-CD81 cells were seeded in 1536-well plates (Greiner Bio, Frickenhausen, Germany). Then, cells were infected with 1×10^3 luciferase-expressing *P. berghei* sporozoites and incubated for a further 48 h. For both control compounds and compound **1**, 50 nL was added in a 1:3 serial dilution of 12 concentrations and incubated for 18 h. Per well, 2 μL of BrightGlo luciferin reagent (Promega, Madison, WI) was added, and luciferase activity was measured with a PerkinElmer Envision multimode plate reader. Values were normalized to maximum inhibition (0.25 μM atovaquone) and minimum inhibition (DMSO). EC_{50} values were calculated with the CDD Vault (Burlingame, CA).

Evaluation in Ex Vivo Clinical Isolates.

The method of evaluating the effect of compound **1** ex vivo was based on a previous study.⁴⁷ Clinical isolates of *P. falciparum* were obtained from patients from the Masafu General Hospital in the Busia district of Uganda, the Tororo District Hospital, and the Patongo Health Center. All patients provided written consent, with the consent for minors provided by a parent/guardian, and assent was provided by patients between 8 and 17 years old. Approval for this study was provided by the Uganda National Council for Science and Technology, the Makerere University Research and Ethics Committee, and the University of California Committee on Human Research. Patients were at least 6 months old and had clinical, but not severe, malaria symptoms and confirmation of infection via Giemsa-stained blood smears. Patients were excluded from the study if they had received treatment for malaria within the past 30 days or were suspected to be infected with other *Plasmodium* species. Prior to patient treatment, 2–5 mL of patient blood was collected in a heparin

collection tube. Parasitemia was determined by counting at least 1000 RBCs on Giemsa-stained blood smears, and only samples with a parasitemia of at least 0.3% were utilized. Blood was washed 3× with RPMI 1640 at 37 °C. Pellets were resuspended in RPMI 1640 supplemented with 25 mM HEPES, 24 mM sodium bicarbonate, 10 µg/mL gentamicin, 0.1 mM hypoxanthine, 0.5% AlbuMAX II (ThermoFisher, Waltham MA) to a hematocrit of 50%. To assess compound efficacy, compound **1** was serially diluted in 96-well plates. As controls, there were wells without compounds and wells without parasites. In addition to the clinical isolates, the lab-adapted strains *P. falciparum* Dd2 and 3D7 are used as controls. Since the clinical isolates are primarily ring stage, 3D7, and Dd2 cultures are synchronized by collecting flow-through from a magnetic MACS column (Miltenyi Biotec, Gaithersburg, MD), as previously described, to isolate ring stage parasites for use in the assay.⁴⁵ Per well, parasites were plated at 0.2% parasitemia and 2% hematocrit, using O+ uninfected RBCs. Plates were incubated for 72 h in 90% N₂, 5% O₂, and 5% CO₂ at 37 °C in a humidified modular chamber (Billups Rothenberg, San Diego, CA, USA). Per well, 100 µL of culture was added to a black 96-well plate with 100 µL lysis buffer (20 mM Tris, 5 mM EDTA, 0.08% Triton X-100, 0.008% saponin, and 0.2 µL/mL SYBR Green I (Thermo Fisher, Waltham, MA)). Plates were mixed and incubated at RT for 1 h, protected from light. Fluorescence was read at 485 nm excitation and 530 nm emission with a FLUOstar Omega multimode microplate reader (BMG LabTech, Cary, NC).

Ring Stage Survival Assay (RSA) and Piperaquine Survival Assay (PSA).

The ring-stage survival assay (RSA) and piperaquine survival assay (PSA) are based on a previously described assay.^{29,31} Briefly, the *P. falciparum* strains 3D7 (MRA-152) and the Cambodian clinical isolates, strains IPC 5188 (MRA-1239), strain IPC 5202 (MRA-1240), and IPC 6261 (MRA-1284) (BEI Resources, Manassas, VA) were cultured in general conditions, as previously described, incubated in a humidified chamber in 90% N₂, 5% O₂, and 5% CO₂ at 37 °C. Parasites were tightly synchronized as via gelatin flotation to enrich in schizonts, and merozoites were allowed to reinvade for 3 h before sorbitol treatment.⁴² Cultures were then diluted to 1% parasitemia and 2% hematocrit for compound treatment. For the RSA, 700 nM of dihydroartemisinin (DHA) was used as a control, and for the PSA, 200 nM piperaquine (PPQ) was used. For both compounds **1** and **16**, 10 × EC₅₀ was used. For the RSA, parasites were treated for 6 h before the compound was washed out and media replenished, whereas the treatment time was 48 h for the PSA. For both assays, parasitemia was determined via Giemsa-stained thin blood smears 72 h after the start of the assay. The parasite survival rate, represented as % survival, is calculated as follows:

$$\% \text{ Survival} = \left(\frac{\text{parasites in compound-treated culture}}{\text{parasites in DMSO-treated culture}} \right) \times 100.$$

Cross Resistance Evaluation.

Compound efficacy was tested in *P. falciparum* lines with mutations to known antiparasitics, and these compounds were used as corresponding controls: AcAS A597 V (compound MMV084978), CARL I1139K (compound GNF179), and PI4K S1320L (compound KDU961). Dd2 was used as a wildtype control, and artemisinin was used as an antiparasitic control compound. The evaluation was performed using the SYBR

Green I assay, as previously described. Briefly, strains were cultivated at 5% hematocrit in media comprised of RPMI with L-glutamine, 38.4 mM HEPES, 3.4 mM NaOH, 0.2% sodium bicarbonate, 0.05 mg/mL gentamicin, 0.2% glucose, 0.2% Albumax (ThermoFisher, Waltham MA), and 4.3% human serum. For screening, compounds were dispensed into a 1536-well black, clear-bottomed plate, and parasites were seeded in screening media (lacking phenol red) to a final hematocrit of 2.5%, final parasitemia of 0.3%, and total volume of 8 μ L. Plates were cultured for 72 h in 93% N₂/3% CO₂/1% CO₂ at 37 °C. Then per well, 2 μ L of SYBR Green I in lysis buffer (20 mM Tris-HCl, 1.6% Triton-X, 0.16% saponin, 5 mM EDTA, and 10 \times SYBR Green I), and plates are incubated in the dark for 24 h at RT. In a 2104 EnVision Multilabel Reader (PerkinElmer, Waltham, MA), fluorescence is detected in 485 nm excitation and 530 nm emission. The assay was performed in a biological duplicate.

Resistance Line Generation.

Four flasks were each inoculated with 1×10^8 blood-stage *P. falciparum* Dd2-B2 parasites at 1% hematocrit. One flask remained untreated, and three were given $1 \times EC_{50}$ of compound **1**, as determined by a SYBR Green I-based assay on primarily ring-stage parasites. Parasitemia was monitored every 48/72 h, and if parasitemia increased, parasite levels were renormalized to 1.2×10^8 parasites per flask.

Minimum Inoculum of Resistance (MIR) Assay.

Blood stage *P. falciparum* Dd2-B2 cultures were maintained in RPMI-1640 media that has been supplemented with 0.225% sodium bicarbonate, 25 mM HEPES, 50 mg/L hypoxanthine, 2 mM L-glutamine, 0.5% (w/v) AlbuMAX II (Invitrogen, Waltham, MA), 10 μ g/mL gentamycin, and at 3% hematocrit in human O+ erythrocytes. Cultures were incubated at 37 °C in 5% CO₂, 5% O₂, and 90% N₂. To determine the EC₁₀ to be used in the minimum inoculum of resistance assay, a flow cytometry-based drug susceptibility assay was performed. Ring-stage *P. falciparum* Dd2-B2 parasites were diluted to 1% hematocrit and 0.2% parasitemia and exposed for 72 h to compound **1** in a 1:2 serial dilution of 10 concentrations, with final DMSO concentration not exceeding 0.5%. As a control, untreated compounds were used. After 72 h, parasite viability was evaluated by staining parasites with SYBR Green I nucleic acid dye and MitoTracker Deep Red mitochondrial vitality dye and quantified with a flow cytometer (Sartorius, Göttingen, Germany). The minimum inoculum of resistance was determined by exposing two different inoculum sizes to $3 \times IC_{10}$ (160.32 nM). One selection was composed of 1.2×10^6 parasites in 12 wells (1.4×10^7 total) and 1×10^7 parasite in 3 wells (3×10^7 total). Following exposure, parasites were monitored via thin blood smear 3 \times per week for 50 days.

Metabolic Stability in Mouse Liver Microsome and Pharmacokinetics Evaluation.

Metabolic Stability in liver microsome data and pharmacokinetic data were obtained as a fee-for-service from UF Scripps Biomedical Research.

Kinetic Solubility.

Kinetic solubility was performed as a fee-for-service from Analiza, Inc., using a miniaturized shake-flask method. Briefly, 50-fold dilutions of the compound were added to the assay buffer (1× PBS, pH 7.4) and incubated with 200 rpm rotary shaking for 24 h at room temperature. The buffer was vacuum-filtered and the filtrate was quantitated by chemiluminescent nitrogen detection (CLND).

Caco-2 Permeability.

Permeability in Caco-2 cells was determined as a fee-for-service by WuXi AppTec Co, Ltd. In brief, Caco-2 cells were seeded onto polyethylene membranes in 96-well plates and treated with 2 μ M compound diluted in Hank's buffered saline solution with 10 mM HEPES, pH 7.4. As controls, 10 μ M digoxin and 2 μ M each of metorolol and nadolol were used. After incubation for 2 h at 37 °C in 5% CO₂, samples were treated with acetonitrile and centrifuged. For the controls, the supernatant was diluted with ultrapure water. Using LC-MS/MS and the peak area ratio of analyte/internal standard, sample, and control compounds were quantified in the starting, donor, and receiver solutions. Afterward, the integrity of the Caco-2 layer was evaluated with a lucifer yellow rejection assay.

In Vivo Evaluation.

Compound **1** was evaluated for efficacy as a prophylactic (single dose through IV injections, 6 h before infection) and therapeutic (4-day Peters test, four doses administered intravenously at 1-, 2-, 3-, and 4- days postinfection). Two doses were tested: 15 and 50 mg/kg. Groups consisted of 5 female Swiss webster mice (Charles River Laboratories International, Inc.), 6 weeks old, and luciferase-expressing rodent malaria parasites, *P. berghe*-ANKA-GFP-Luc SMcon (*P. berghe*^{Luc}) were used.⁴⁸ *P. berghe*^{Luc} parasites come from infected *Anopheles stephensi* mosquitos raised at the SporoCore, University of Georgia. As controls, an uninfected group, an infected and untreated group (injected only with 200 μ L of the vehicle resuspension: 27% DMSO, 1% methylcellulose, 0.5% Tween-80, and 71.5% ultrapure water), and a group treated with the known antiplasmodial compound GNF179 (Chemstep, CS-2796) were used. Compound **1** was dissolved in a vehicle containing 27% DMSO, 1% methylcellulose, 0.5% Tween-80, and 71.5% ultrapure water, and GNF179 was resuspended in 34% DMSO, 25% PEG400, 5% Tween-80, and 36% saline. For the prophylactic model, mice were infected with 10⁵ *P. berghe*^{Luc} sporozoites by IV injection (parasites resuspended in 200 μ L of DMEM media (DMEM media supplemented with 5% FBS, 146 mg/mL glutamine, 500 units of penicillin, and 500 μ g/mL streptomycin)). For the therapeutic model, mice were infected with 10⁷ infected RBCs (200 μ L of cryopreserved solution of infected RBC) by IP injection (from a cryopreserved infected blood solution containing ~1000 μ L mouse infected RBC (10% parasitemia) resuspended in 300 μ L heparin (1 unit/ μ L) and 4000 μ L of freezing solution (15% glycerol, 2.5% FBS and 80% RPMI media)). The parasitemia was monitored from 2 days post-infection (DPI) to 16 DPI by flow cytometry (BD FACSCanto II Flow Cytometry System and FlowJo Software), 6.4 μ L of whole blood obtained from the tail of each mouse was resuspended in 320 μ L PBS 1× with heparin (0.5 units/ml), the sample was then stained with PBS-SYBR Green I 0.125× (S7567, Invitrogen) for 30 min at 37 °C, and the readouts

were performed by flow cytometry. The images were obtained through an In Vivo Imaging Instrument (IVIS); mice anesthetized with isoflurane in the vaporizer system (Caliper Life Sciences, XGI-8, gas anesthesia system) were imaged during 120 s using IVIS equipment (IVIS Lumina LT Series III, PerkinElmer, Waltham, MA, and Living Image 4.3.1 Software). In vivo assays were performed following an approved protocol (S13013) by the Institutional Animal Care and Use Committee (IACUC) from UCSD.

Supplementary Material

Refer to Web version on PubMed Central for supplementary material.

ACKNOWLEDGMENTS

We would like to thank the Thermo Fisher Scientific Center for Multiplexed Proteomics at Harvard Medical School (<http://tcmp.hms.edu>), as well as the lab of David Fidock of Columbia University Irving Medical Center. This work was supported by a grant from NIH AI172066 (to DC, NSG, and EAW). The following reagent was obtained through BEI Resources, NIAID, NIH: *Plasmodium falciparum*, Strain Dd2, MRA-156, contributed by Thomas E. Wellems. The following reagent was obtained through BEI Resources, NIAID, NIH: *Plasmodium falciparum*, Strain 3D7, MRA-102, contributed by Daniel J. Carucci. The following reagents were obtained through BEI Resources, NIAID, NIH: *Plasmodium falciparum*, Strain IPC_6261, MRA-1284; *Plasmodium falciparum*, Strain IPC 5202, MRA-1240; and *Plasmodium falciparum*, Strain IPC 5188, MRA-1239; all of which were contributed by Didier Ménard. Infected mosquitos from the SporoCore, University of Georgia, and in vivo assays were supported by the grants from NIH 1R01AI152533 (EAW), R01AI169892, and from Bill and Melinda Gates Foundation grant number INV-039628 (EAW).

ABBREVIATIONS

ACT	artemisinin combination therapy
DHA	dihydroartemisinin
DPI	days post infection
EC₅₀	half maximal effective concentration
HPI	hours post invasion
IC₅₀	half maximal inhibitory concentration
MIR	minimum inoculum of resistance
<i>Pf</i>	<i>Plasmodium falciparum</i>
PPQ	piperaquine
PRR	parasite reduction ratio
PSA	piperaquine survival assay
RBC	red blood cell
RI	resistance index
RSA	ring stage survival assay
RT	room temperature

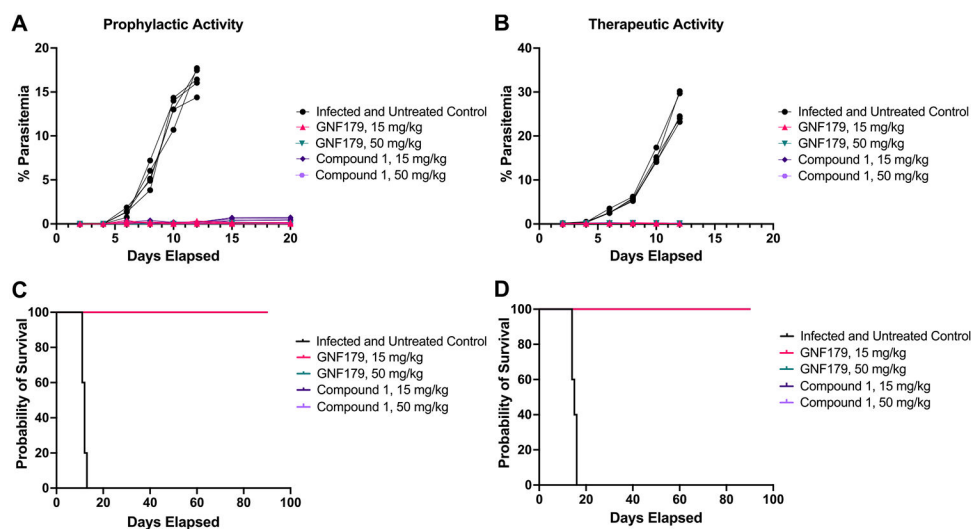
SD	standard deviation
SEM	standard error of the mean
SI	selectivity index

REFERENCES

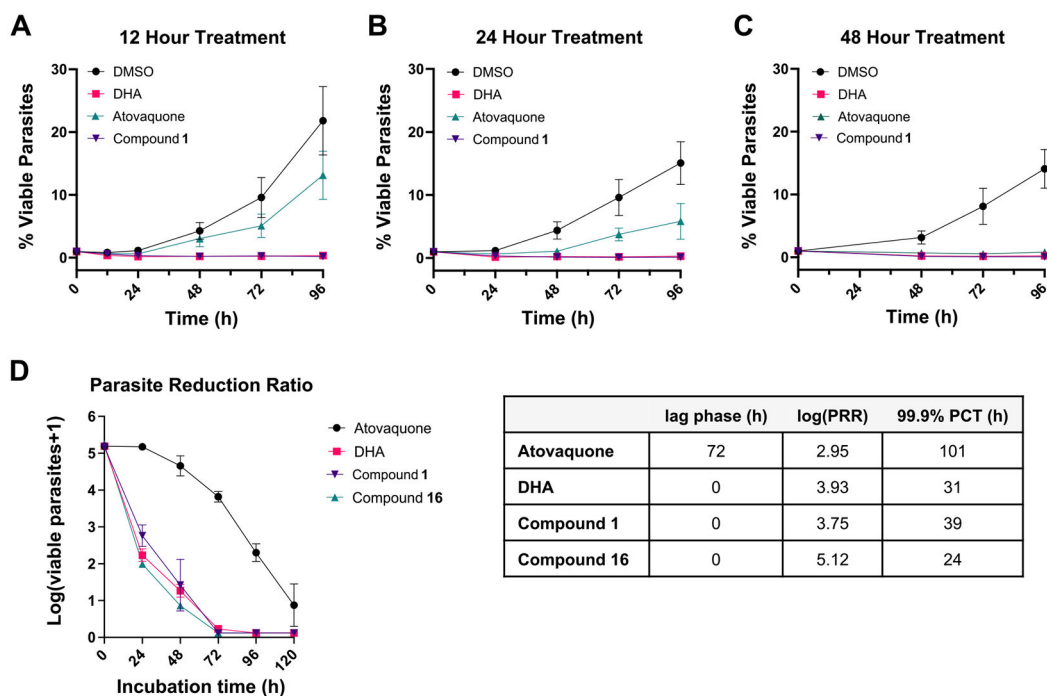
- (1). World Malaria Report 2022; World Health Organization, 2022.
- (2). Uwimana A; Legrand E; Stokes BH; Ndikumana JM; Warsame M; Umulisa N; Ngamiye D; Munyaneza T; Mazarati JB; Munguti K; et al. Emergence and clonal expansion of in vitro artemisinin-resistant *Plasmodium falciparum* kelch13 R561H mutant parasites in Rwanda. *Nat. Med* 2020, 26 (10), 1602–1608. [PubMed: 32747827]
- (3). Diallo BN; Swart T; Hoppe HC; Tastan Bishop O; Lobb K Potential repurposing of four FDA approved compounds with antiplasmodial activity identified through proteome scale computational drug discovery and in vitro assay. *Sci. Rep* 2021, 11 (1), 1413. [PubMed: 33446838]
- (4). Ayala-Aguilera CC; Valero T; Lorente-Macias A; Baillache DJ; Croke S; Unciti-Broceta A Small Molecule Kinase Inhibitor Drugs (1995–2021): Medical Indication, Pharmacology, and Synthesis. *J. Med. Chem* 2022, 65 (2), 1047–1131. [PubMed: 34624192]
- (5). Ferguson FM; Gray NS Kinase inhibitors: the road ahead. *Nat. Rev. Drug Discov* 2018, 17 (5), 353–377. [PubMed: 29545548]
- (6). Derbyshire ER; Zuzarte-Luis V; Magalhaes AD; Kato N; Sanschagrin PC; Wang J; Zhou W; Miduturu CV; Mazitschek R; Sliz P; et al. Chemical interrogation of the malaria kinome. *Chembiochem* 2014, 15 (13), 1920–1930. [PubMed: 25111632]
- (7). Burrows JN; Duparc S; Gutteridge WE; Hooft van Huijsduijnen R; Kaszubska W; Macintyre F; Mazzuri S; Mohrle JJ; Wells TNC New developments in anti-malarial target candidate and product profiles. *Malar J.* 2017, 16 (1), 26. [PubMed: 28086874]
- (8). Adderley J; Williamson T; Doerig C Parasite and Host Erythrocyte Kinomics of *Plasmodium* Infection. *Trends Parasitol* 2021, 37 (6), 508–524. [PubMed: 33593681]
- (9). Arendse LB; Wyllie S; Chibale K; Gilbert IH *Plasmodium* Kinases as Potential Drug Targets for Malaria: Challenges and Opportunities. *ACS Infect Dis* 2021, 7 (3), 518–534. [PubMed: 33590753]
- (10). Cabrera DG; Horatscheck A; Wilson CR; Basarab G; Eyermann CJ; Chibale K Plasmodial Kinase Inhibitors: License to Cure? *J. Med. Chem* 2018, 61 (18), 8061–8077. [PubMed: 29771541]
- (11). Ong HW; Adderley J; Tobin AB; Drewry DH; Doerig C Parasite and host kinases as targets for antimalarials. *Expert Opin. Ther. Targets* 2023, 27 (2), 151–169, DOI: 10.1080/14728222.2023.2185511. [PubMed: 36942408]
- (12). Wang B; Wu H; Hu C; Wang H; Liu J; Wang W; Liu Q An overview of kinase downregulators and recent advances in discovery approaches. *Signal Transduct Target Ther* 2021, 6 (1), 423. [PubMed: 34924565]
- (13). Liu Y; Gray NS Rational design of inhibitors that bind to inactive kinase conformations. *Nat. Chem. Biol* 2006, 2 (7), 358–364. [PubMed: 16783341]
- (14). Schneider EV; Bottcher J; Huber R; Maskos K; Neumann L Structure-kinetic relationship study of CDK8/CycC specific compounds. *Proc. Natl. Acad. Sci. U. S. A* 2013, 110 (20), 8081–8086. [PubMed: 23630251]
- (15). Copeland RA; Pompliano DL; Meek TD Drug-target residence time and its implications for lead optimization. *Nat. Rev. Drug Discov* 2006, 5 (9), 730–739. [PubMed: 16888652]
- (16). Kesely KR; Pantaleo A; Turrini FM; Olupot-Olupot P; Low PS Inhibition of an Erythrocyte Tyrosine Kinase with Imatinib Prevents *Plasmodium falciparum* Egress and Terminates Parasitemia. *PLoS One* 2016, 11 (10), No. e0164895. [PubMed: 27768734]
- (17). Ong HW; Truong A; Kwarcinski F; de Silva C; Avalani K; Havener TM; Chirgwin M; Galal KA; Willis C; Kramer A; et al. Discovery of potent *Plasmodium falciparum* protein kinase 6 (Pfk6)

- inhibitors with a type II inhibitor pharmacophore. *Eur. J. Med. Chem* 2023, 249, No. 115043. [PubMed: 36736152]
- (18). Dery V; Duah NO; Ayanful-Torgby R; Matrevi SA; Anto F; Quashie NB An improved SYBR Green-1-based fluorescence method for the routine monitoring of *Plasmodium falciparum* resistance to anti-malarial drugs. *Malar J.* 2015, 14, 481. [PubMed: 26625907]
- (19). Choi Y; Syeda F; Walker JR; Finerty PJ Jr.; Cuerrier D; Wojciechowski A; Liu Q; Dhe-Paganon S; Gray NS Discovery and structural analysis of Eph receptor tyrosine kinase inhibitors. *Bioorg. Med. Chem. Lett* 2009, 19 (15), 4467–4470. [PubMed: 19553108]
- (20). Chiodi D; Ishihara Y "Magic Chloro": Profound Effects of the Chlorine Atom in Drug Discovery. *J. Med. Chem* 2023, 66 (8), 5305–5331. [PubMed: 37014977]
- (21). Lin FY; MacKerell AD Jr. Do Halogen-Hydrogen Bond Donor Interactions Dominate the Favorable Contribution of Halogens to Ligand-Protein Binding? *J. Phys. Chem. B* 2017, 121 (28), 6813–6821. [PubMed: 28657759]
- (22). Zhu Z; Xu Z; Zhu W Interaction Nature and Computational Methods for Halogen Bonding: A Perspective. *J. Chem. Inf Model* 2020, 60 (6), 2683–2696. [PubMed: 32453594]
- (23). Meister S; Plouffe DM; Kuhlen KL; Bonamy GM; Wu T; Barnes SW; Bopp SE; Borboa R; Bright AT; Che J; et al. Imaging of *Plasmodium* liver stages to drive next-generation antimalarial drug discovery. *Science* 2011, 334 (6061), 1372–1377. [PubMed: 22096101]
- (24). Peters W. The chemotherapy of rodent malaria, XXII. The value of drug-resistant strains of *P. berghei* in screening for blood schizontocidal activity. *Ann. Trop. Med. Parasitol* 1975, 69 (2), 155–171. [PubMed: 1098584]
- (25). Somsak V; Srichairatanakool S; Yuthavong Y; Kamchonwongpaisan S; Uthairipibull C Flow cytometric enumeration of *Plasmodium berghei*-infected red blood cells stained with SYBR Green I. *Acta Trop* 2012, 122 (1), 113–118. [PubMed: 22222185]
- (26). Sanz LM; Crespo B; De-Cozar C; Ding XC; Llergo JL; Burrows JN; Garcia-Bustos JF; Gamo FJP *falciparum* in vitro killing rates allow to discriminate between different antimalarial mode-of-action. *PLoS One* 2012, 7 (2), No. e30949. [PubMed: 22383983]
- (27). Klonis N; Xie SC; McCaw JM; Crespo-Ortiz MP; Zaloumis SG; Simpson JA; Tilley L Altered temporal response of malaria parasites determines differential sensitivity to artemisinin. *Proc. Natl. Acad. Sci. U. S. A* 2013, 110 (13), 5157–5162. [PubMed: 23431146]
- (28). Arieu F; Witkowski B; Amaratunga C; Beghain J; Langlois AC; Khim N; Kim S; Duru V; Bouchier C; Ma L; et al. A molecular marker of artemisinin-resistant *Plasmodium falciparum* malaria. *Nature* 2014, 505 (7481), 50–55. [PubMed: 24352242]
- (29). Witkowski B; Amaratunga C; Khim N; Sreng S; Chim P; Kim S; Lim P; Mao S; Sopha C; Sam B; et al. Novel phenotypic assays for the detection of artemisinin-resistant *Plasmodium falciparum* malaria in Cambodia: in-vitro and ex-vivo drug-response studies. *Lancet Infect Dis* 2013, 13 (12), 1043–1049. [PubMed: 24035558]
- (30). Witkowski B; Khim N; Chim P; Kim S; Ke S; Kloeung N; Chy S; Duong S; Leang R; Ringwald P; et al. Reduced artemisinin susceptibility of *Plasmodium falciparum* ring stages in western Cambodia. *Antimicrob. Agents Chemother* 2013, 57 (2), 914–923. [PubMed: 23208708]
- (31). Duru V; Khim N; Leang R; Kim S; Domergue A; Kloeung N; Ke S; Chy S; Eam R; Khean C; et al. *Plasmodium falciparum* dihydroartemisinin-piperaquine failures in Cambodia are associated with mutant K13 parasites presenting high survival rates in novel piperaquine in vitro assays: retrospective and prospective investigations. *BMC Med.* 2015, 13, 305. [PubMed: 26695060]
- (32). Leang R; Taylor WR; Bouth DM; Song L; Tarning J; Char MC; Kim S; Witkowski B; Duru V; Domergue A; et al. Evidence of *Plasmodium falciparum* Malaria Multidrug Resistance to Artemisinin and Piperaquine in Western Cambodia: Dihydroartemisinin-Piperaquine Open-Label Multicenter Clinical Assessment. *Antimicrob. Agents Chemother* 2015, 59 (8), 4719–4726. [PubMed: 26014949]
- (33). Summers RL; Pasaje CFA; Pisco JP; Striepen J; Luth MR; Kumpornsin K; Carpenter EF; Munro JT; Lin; Plater A; et al. Chemogenomics identifies acetyl-coenzyme A synthetase as a target for malaria treatment and prevention. *Cell Chem. Biol* 2022, 29 (2), 191–201.e8. [PubMed: 34348113]

- (34). LaMonte G; Lim MY; Wree M; Reimer C; Nachon M; Corey V; Gedeck P; Plouffe D; Du A; Figueroa N; et al. Mutations in the Plasmodium falciparum Cyclic Amine Resistance Locus (PFCARL) Confer Multidrug Resistance. *mBio* 2016, 7, 4.
- (35). McNamara CW; Lee MC; Lim CS; Lim SH; Roland J; Simon O; Yeung BK; Chatterjee AK; McCormack SL; Manary MJ; et al. Targeting Plasmodium PI(4)K to eliminate malaria. *Nature* 2013, 504 (7479), 248–253. [PubMed: 24284631]
- (36). Cowell AN; Istvan ES; Lukens AK; Gomez-Lorenzo MG; Vanaerschot M; Sakata-Kato T; Flannery EL; Magistrado P; Owen E; Abraham M; et al. Mapping the malaria parasite druggable genome by using in vitro evolution and chemogenomics. *Science* 2018, 359 (6372), 191–199. [PubMed: 29326268]
- (37). Duffey M; Blasco B; Burrows JN; Wells TNC; Fidock DA; Leroy D Assessing risks of Plasmodium falciparum resistance to select next-generation antimalarials. *Trends Parasitol* 2021, 37 (8), 709–721. [PubMed: 34001441]
- (38). Munoz L. Non-kinase targets of protein kinase inhibitors. *Nat. Rev. Drug Discov* 2017, 16 (6), 424–440. [PubMed: 28280261]
- (39). Trager W; Jensen JB Human malaria parasites in continuous culture. *Science* 1976, 193 (4254), 673–675. [PubMed: 781840]
- (40). Clements RL; Strelva V; Dumoulin P; Huang W; Owens E; Raj DK; Burleigh B; Llinas M; Winzeler EA; Zhang Q; et al. A Novel Antiparasitic Compound Kills Ring-Stage Plasmodium falciparum and Retains Activity Against Artemisinin-Resistant Parasites. *J. Infect Dis* 2020, 221 (6), 956–962. [PubMed: 31616928]
- (41). Dluzewski AR; Ling IT; Rangachari K; Bates PA; Wilson RJ A simple method for isolating viable mature parasites of Plasmodium falciparum from cultures. *Trans R Soc. Trop Med. Hyg* 1984, 78 (5), 622–624. [PubMed: 6095494]
- (42). Jensen JB Concentration from continuous culture of erythrocytes infected with trophozoites and schizonts of Plasmodium falciparum. *Am. J. Trop Med. Hyg* 1978, 27 (6), 1274–1276. [PubMed: 365006]
- (43). Lambros C; Vanderberg JP Synchronization of Plasmodium falciparum erythrocytic stages in culture. *J. Parasitol* 1979, 65 (3), 418–420. [PubMed: 383936]
- (44). Wright AE; Collins JE; Roberts B; Roberts JC; Winder PL; Reed JK; Diaz MC; Pomponi SA; Chakrabarti D Antiplasmodial Compounds from Deep-Water Marine Invertebrates. *Mar. Drugs* 2021, 19 (4), 179. [PubMed: 33805935]
- (45). Mata-Cantero L; Lafuente MJ; Sanz L; Rodriguez MS Magnetic isolation of Plasmodium falciparum schizonts iRBCs to generate a high parasitaemia and synchronized in vitro culture. *Malar J.* 2014, 13, 112. [PubMed: 24655321]
- (46). Antonova-Koch Y; Meister S; Abraham M; Luth MR; Otilie S; Lukens AK; Sakata-Kato T; Vanaerschot M; Owen E; Jado JC; et al. Open-source discovery of chemical leads for next-generation chemoprotective antimalarials. *Science* 2018, 362, 6419.
- (47). Tumwebaze PK; Katairo T; Okitwi M; Byaruhanga O; Orena S; Asua V; Duval Saint M; Legac J; Chelebieva S; Ceja FG; et al. Drug susceptibility of Plasmodium falciparum in eastern Uganda: a longitudinal phenotypic and genotypic study. *Lancet Microbe* 2021, 2 (9), e441–e449. [PubMed: 34553183]
- (48). Janse CJ; Franke-Fayard B; Mair GR; Ramesar J; Thiel C; Engelmann S; Matuschewski K; van Gemert GJ; Sauerwein RW; Waters AP High efficiency transfection of Plasmodium berghei facilitates novel selection procedures. *Mol. Biochem. Parasitol* 2006, 145 (1), 60–70. [PubMed: 16242190]

**Figure 1.**

Compound **1** prevents blood-stage malaria infection when applied prophylactically (A, C) and cures infection when given therapeutically (B, D) at 15 and 50 mg/kg. For A and C, mice (infected and untreated control group) were pretreated with vehicle alone or given a single 15 or 50 mg/kg dose of a control compound, GNF179,²³ or compound **1** via IV injection in the vehicle. After 6 h groups of 5 mice were infected with 10^5 *P. berghei*^{Luc} sporozoites²³ suspended in DMEM media via IV injection. For B and D, mice were infected with 10^7 fresh *P. berghei*^{Luc} iRBCs suspended in cryopreservation solution via IP infection and then treated afterward at 1, 2, 3, and 4 days post-infection via IV injection in the standard Peter's test²⁴ using compounds described above. Parasitemia was determined by flow cytometry²⁵ at the indicated days for A and B. Survival is shown in C and D.

**Figure 2.**

Killing profile of compound 1 in blood-stage *P. falciparum*. Fast-acting DHA and slow-acting atovaquone are controls. (A–C) Flow-cytometry-based assay evaluated parasite viability after treatment for 12 (A), 24 (B), and 48 (C) hours. Graphs depict the average of 3 biological replicates \pm SEM (D) *P. falciparum* parasite reduction ratio of both compounds **1** and **16** with the accompanying table. The graph presents data from 2 biological replicates \pm SEM. The lag phase is the time before the maximal killing rate. PRR (parasite reduction ratio) is the reduction of viable parasites over one life cycle. 99.9% PCT (parasite clearance time) is the time required to clear the initial parasite load by 3-log units.

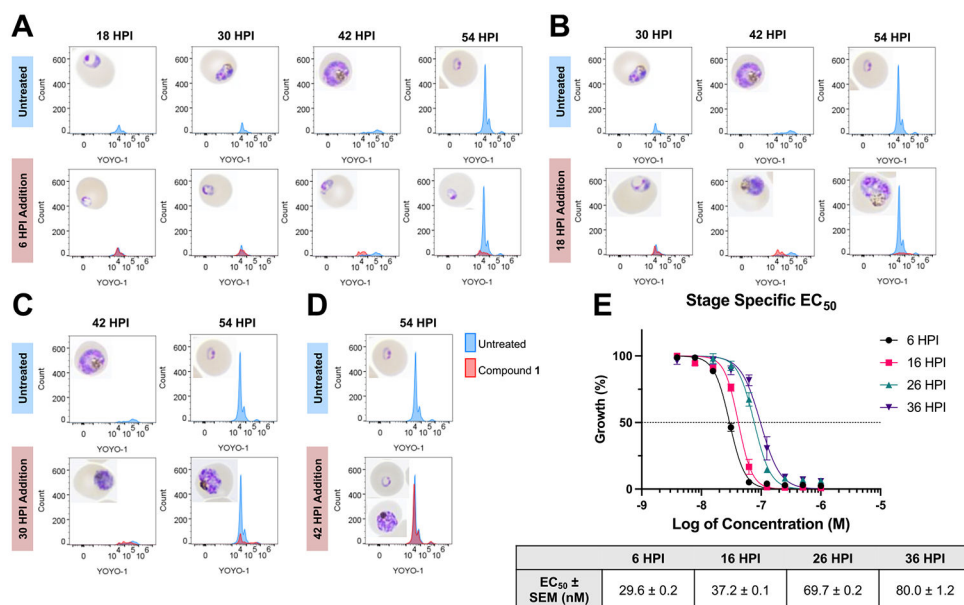


Figure 3. Stage specific activity of compound **1**. (A–D) Flow cytometry to detect DNA replication and Giemsa-stained thin blood smears to monitor morphology, with treatment at 6 HPI (A), 18 HPI (B), 30 HPI (C), and 42 HPI (D). Histograms representative of 3 biological replicates. (E) Stage specific EC_{50} of compound **1** confirms increased potency in early asexual stage. Graph reflects 3 biological replicates \pm SEM.

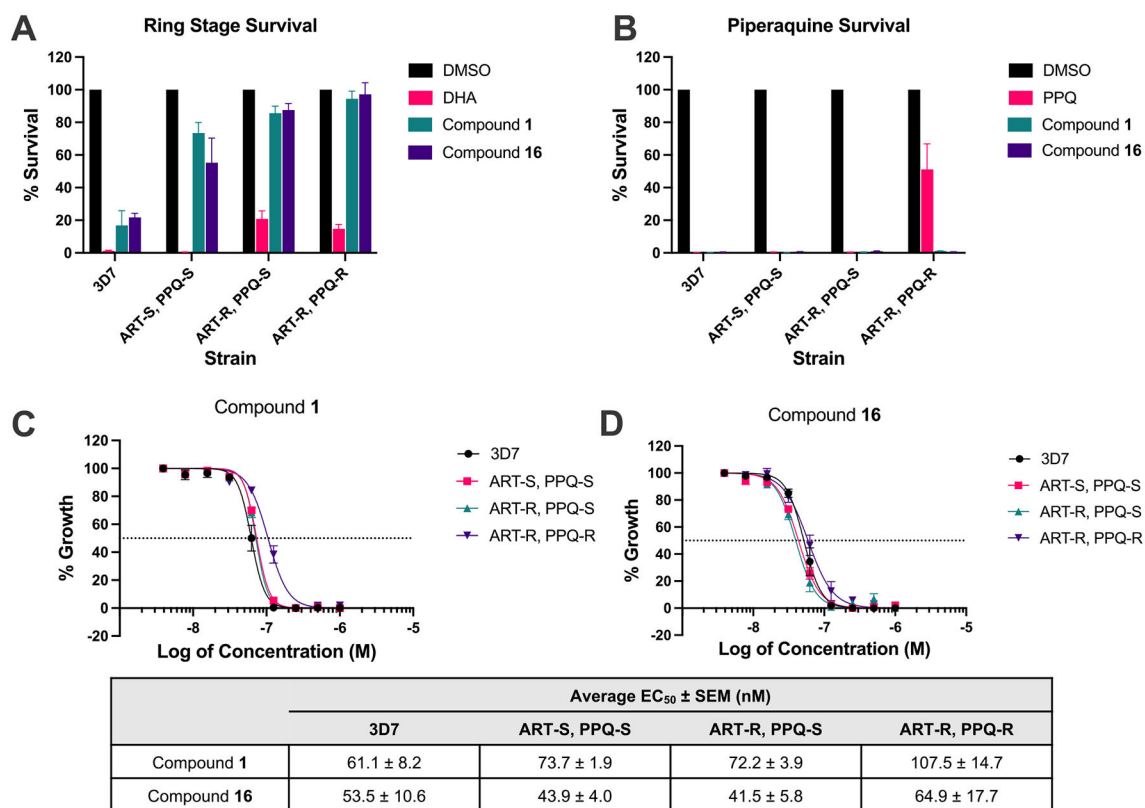
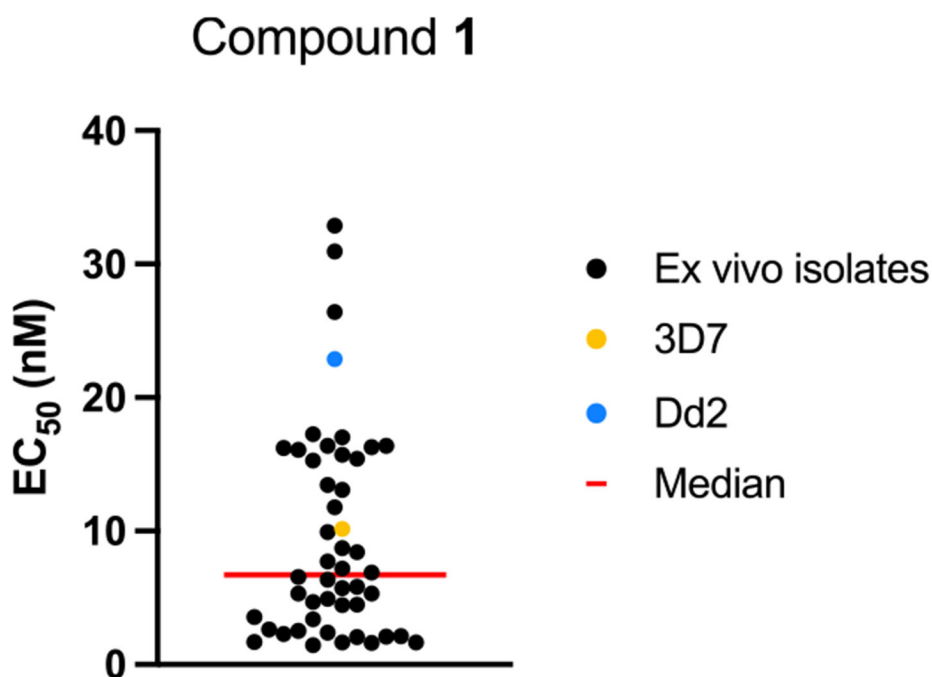
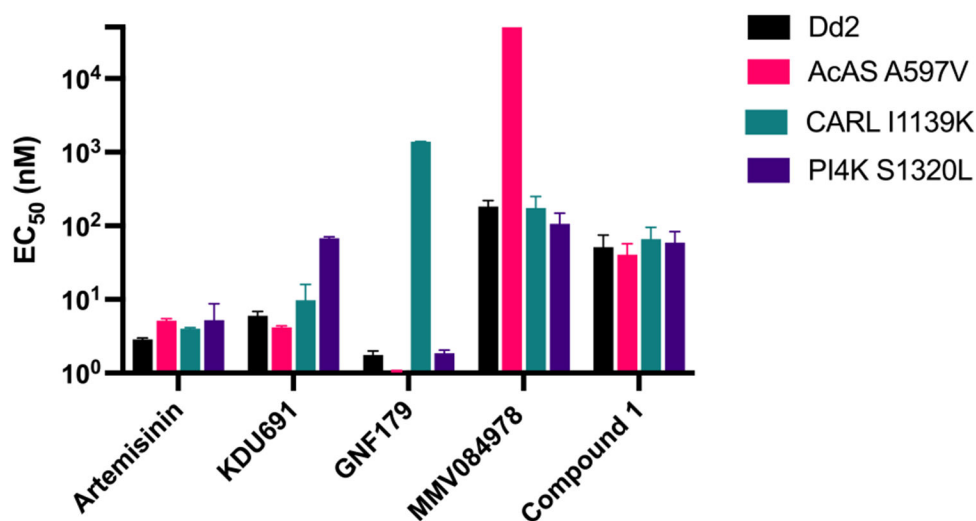


Figure 4. Compounds **1** and **16** are effective in artemisinin and piperaquine resistant isolates. Parasite lines are resistant (–R) or sensitive (–S) to artemisinin (ART) or piperaquine (PPQ). (A) Ring Stage Survival Assay and (B) Piperaquine Survival Assay graphs reflect average % survival ± SEM of 3 biological replicates. (C, D) EC₅₀ determination, graphs depict average ± SEM of 3 biological replicates.



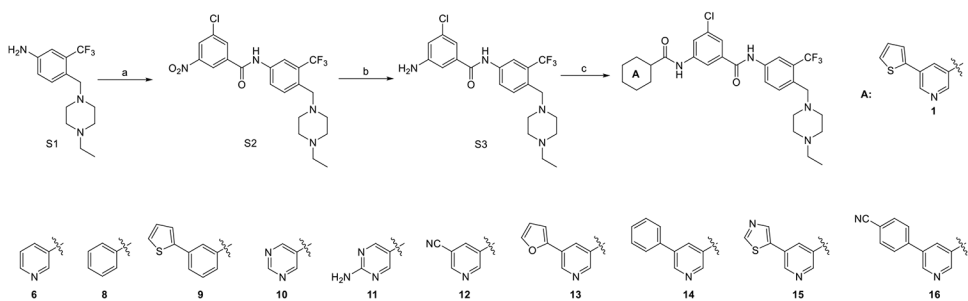
Sample	Average EC ₅₀ ± SEM (nM)
<i>Ex Vivo Isolates</i>	9.2 ± 1.2
Dd2	22.9 ± 5.4
3D7	10.2 ± 3.1

Figure 5. Compound 1 maintains potency in Ugandan field isolates. Compound 1 was evaluated against *P. falciparum* ex vivo isolates from patients in the Ugandan towns of Patongo, Tororo, and Busiu. Ring stage Dd2 and 3D7 were also evaluated for comparison with lab-adapted strains. Graph shows individual EC₅₀ values of ex vivo isolates and average of Dd2 and 3D7 EC₅₀ values from biological triplicates.



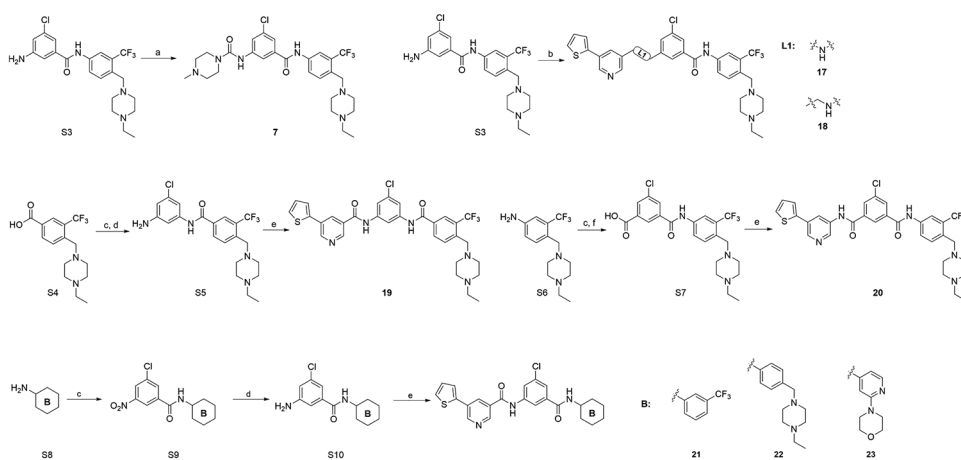
Compound	Average EC ₅₀ (nM) ± SEM			
	Dd2	AcAS A597V	CARL I1139K	PI4K S1320L
Artemisinin	2.9 ± 0.2	5.1 ± 0.4	4.0 ± 0.2	5.2 ± 3.5
KDU691 (imidazopyrazines)	6.0 ± 0.9	4.2 ± 0.2	9.8 ± 6.3	67.6 ± 3.5
GNF179 (imidazolopiperazines)	1.8 ± 0.2	1.1 ± 0.0	1385.0 ± 15.0	1.9 ± 0.2
MMV084978	182.5 ± 37.5	> 50,000	173.8 ± 76.2	106.3 ± 42.8
Compound 1	51.2 ± 24.0	40.5 ± 16.9	65.8 ± 29.3	59.2 ± 24.1

Figure 6. Compound 1 displays no cross-resistance in *P. falciparum* strains resistant to known antiplasmodials. Results displayed are the average of 2 biological replicates ± SEM.



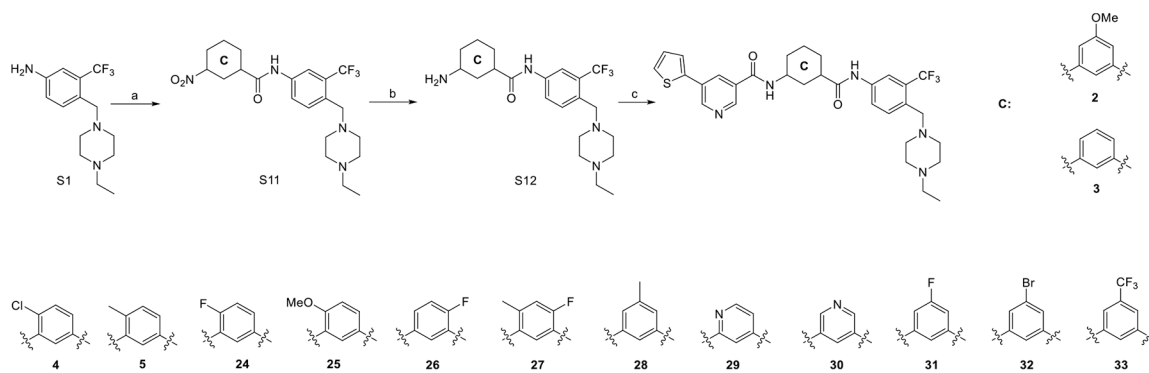
Scheme 1. Synthesis of Compounds 1, 6, and 8–16

^aReagents and conditions: (a) 3-chloro-5-nitrobenzoic acid, HATU, DIPEA, DMF, 25 °C, 1 h; (b) Fe, NH₄Cl, EtOH/H₂O, 80 °C, 5 h; (c) acid or acyl chloride, coupling condition.

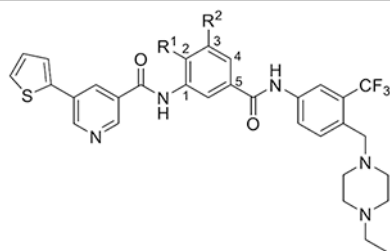


Scheme 2. Synthesis of Compounds 7, 17–23

^aReagents and conditions: (a) Triphosgene, 1-methylpiperazine, DIPEA, CH_2Cl_2 , 0–25 °C (b) **17**: 3-bromo-5-(thiophen-2-yl) pyridine, K_3PO_4 , *t*-BuBrettPhos Pd G3, *t*-BuBrettPhos, 2Me-THF, 80 °C **18**: 5-(thiophen-2-yl)nicotinaldehyde, NaBH_3CN , AcOH, 25 °C, 2 h; (c) 3-chloro-5-nitrobenzoic acid, HATU, DIPEA, DMF, 25 °C; (d) Fe, NH_4Cl , EtOH/ H_2O , 75 °C, 3 h; (e) 5-(thiophen-2-yl)nicotinoyl chloride, DIPEA, DMF, 25 °C. (f) NaOH, THF/MeOH/ H_2O , 25 °C.

**Scheme 3. Synthesis of Compounds 2–5, 24–33**

^aReagents and conditions: (a) 5-nitrobenzoic acid derivatives, HATU, DIPEA, DMF, 25 °C, 12 h; (b) Fe, NH₄Cl, EtOH/H₂O, 75 °C, 2 h; (c) acid or acyl chloride, coupling condition.

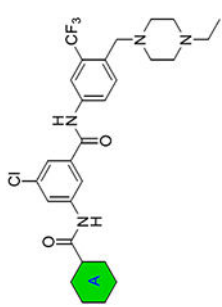



Table 1.Central Ring Substitutions Decouple Human EphA2 Activity from Antiplasmodial Activity^{a,b}

compound	R ¹	R ²	human EphA2 IC ₅₀ (nM) ± SD	<i>P. falciparum</i> Dd2 EC ₅₀ (nM) ± SD
1	H	-Cl	>10,000	80 ± 8
2	H	-OCH ₃	>10,000	341 ± 47
3	H	H	6730 ± 5530	479 ± 98
4	-Cl	H	52 ± 13	770 ± 182
5	-CH ₃	H	11 ± 0.3	3910 ± 1630

^aEphA2 activity determined by SelectScreen kinase profiling.^bAntiplasmodial activity determined by SYBR Green I-based proliferation assay in asynchronous parasites.

Table 2.

SAR Study of the Solvent-Exposed Region

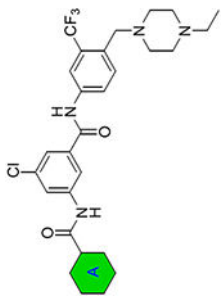
ID	A	Antiplasmodial Activity				Cytotoxicity			
		Dd2 EC ₅₀ (nM)	3D7 EC ₅₀ (nM)	RP ^a	HepG2 EC ₅₀ (nM)	SP ^b	MCF7 EC ₅₀ (nM)	SI ^c	
1		58 ± 5	42 ± 8	1.4	2590 ± 84	45	3510 ± 727	61	
6		147 ± 23	127 ± 13	1.2	10400 ± 140	71	11000 ± 1810	75	
7		1230 ± 123	2120 ± 350	0.6	14000 ± 2030	11	18800 ± 521	15	
8		493 ± 73	361 ± 8	1.4	7240 ± 1360	15	6070 ± 133	12	
9		253 ± 41	196 ± 13	1.3	5460 ± 302	22	8360 ± 812	33	
10		520 ± 66	395 ± 24	1.3	17300 ± 2430	33	15300 ± 699	29	

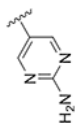
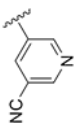
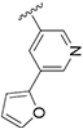
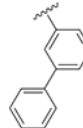
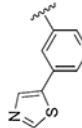
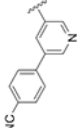
Author Manuscript

Author Manuscript

Author Manuscript

Author Manuscript



ID	A	Antiplasmodial Activity				Cytotoxicity			
		Dd2 EC ₅₀ (nM)	3D7 EC ₅₀ (nM)	R ₁ ^a	HepG2 EC ₅₀ (nM)	SI ^b	MCF7 EC ₅₀ (nM)	SI ^c	
11		709 ± 118	378 ± 62	1.9	19200 ± 604	27	13700 ± 349	19	
12		191 ± 12	186 ± 9	1.0	11000 ± 758	58	7580 ± 165	40	
13		51 ± 5	58 ± 8	0.9	5410 ± 228	106	6490 ± 637	127	
14		50 ± 3	41 ± 4	1.2	3290 ± 175	66	4350 ± 811	87	
15		56 ± 7	74 ± 1	0.8	6080 ± 928	109	8140 ± 1600	145	
16		36 ± 3	36 ± 2	1.0	1460 ± 185	41	2190 ± 292	61	

^aResistance Index (RI) = *P. falciparum* Dd2 EC₅₀/*P. falciparum* 3D7 EC₅₀.^bSelectivity Index (SI) = HepG2 EC₅₀/*P. falciparum* Dd2 EC₅₀.

^cSelectivity Index (SI) = MCF7 EC50/*P. falciparum* Dd2 EC50. Antiplasmodial activity determined by SYBR Green I-based proliferation assay in ring stage parasites. Cytotoxicity evaluated by MTS-based viability assay.

Author Manuscript

Author Manuscript

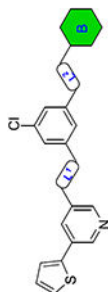
Author Manuscript

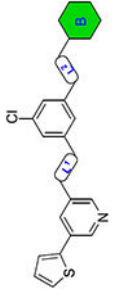
Author Manuscript

Table 3.

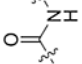
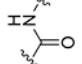
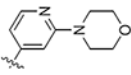
SAR Study of Linker and Tail

ID	L ¹	L ²	B	Antiplasmodial Activity				Cytotoxicity			
				Dd2 EC ₅₀ (nM)	3D7 EC ₅₀ (nM)	Rt ^a	HepG2 EC ₅₀ (nM)	SI ^b	MCF7 EC ₅₀ (nM)	SI ^c	
1				58 ± 5	42 ± 8	1.4	2590 ± 84	45	3510 ± 727	61	
17				296 ± 23	253 ± 21	1.2	3620 ± 670	12	5530 ± 331	19	
18				344 ± 52	310 ± 42	1.1	5590 ± 198	16	8330 ± 1070	24	
19				104 ± 12	73 ± 3	1.4	9160 ± 1340	88	7030 ± 488	68	
20				109 ± 17	82 ± 9	1.3	4240 ± 461	39	5360 ± 473	49	
21				1110 ± 154	541 ± 106	2.1	>20000	>18	>20000	>18	
22				81 ± 4	76 ± 3	1.1	8770 ± 1090	108	10300 ± 1090	127	





Chemical structure of compound 23: A complex molecule featuring a central benzene ring with a chlorine atom at the 4-position. It is substituted with a 2-thienyl group at the 1-position, a 2-pyridinyl group at the 2-position, and a 2-(1,3,4-oxadiazol-5-yl)ethyl group at the 3-position. The oxadiazole ring is further substituted with a 1,3,4-oxadiazol-5-yl group.

ID	Antiplasmodial Activity					Cytotoxicity				
	L ¹	L ²	B	Dd2 EC ₅₀ (nM)	3D7 EC ₅₀ (nM)	RI ^a	HepG2 EC ₅₀ (nM)	SI ^b	MCF7 EC ₅₀ (nM)	SI ^c
23				739 ± 4	700 ± 17	1.1	>20000	27	14700 ± 1400	20

^aResistance Index (RI) = *P. falciparum* Dd2 EC₅₀/*P. falciparum* 3D7 EC₅₀.

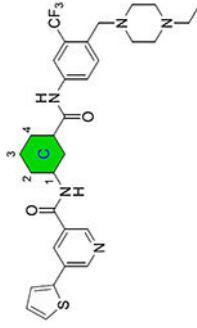
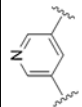
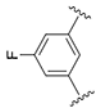
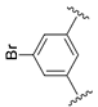
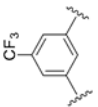
^bSelectivity Index (SI) = HepG2 EC₅₀/*P. falciparum* Dd2 EC₅₀.

^cSelectivity Index (SI) = MCF7 EC₅₀/*P. falciparum* Dd2 EC₅₀. Antiplasmodial activity determined by SYBR Green I-based proliferation assay in ring stage parasites. Cytotoxicity evaluated by MTS-based viability assay.

Table 4.

SAR Study of the Central Ring

ID	C	Antiplasmodial Activity				Cytotoxicity			
		Dd2 EC ₅₀ (nM)	3D7 EC ₅₀ (nM)	RI ^a	HepG2 EC ₅₀ (nM)	SI ^b	MCF7 EC ₅₀ (nM)	SI ^c	
1		58 ± 5	42 ± 8	1.4	2590 ± 84	45	3510 ± 727	61	
24		1320 ± 79	763 ± 51	1.7	3170 ± 332	2.4	5100 ± 952	3.9	
25		1540 ± 252	821 ± 18	1.9	3240 ± 496	2.1	5060 ± 978	3.3	
26		981 ± 27	491 ± 26	2.0	6710 ± 907	6.8	10800 ± 1690	11	
27		1580 ± 108	1460 ± 63	1.1	4050 ± 335	2.6	6910 ± 640	4.4	
28		372 ± 37	235 ± 34	1.6	3200 ± 238	8.6	5220 ± 517	14	

ID	C	Antiplasmodial Activity			Cytotoxicity		
		Dd2 EC ₅₀ (nM)	3D7 EC ₅₀ (nM)	RI ^a	HepG2 EC ₅₀ (nM)	MCF7 EC ₅₀ (nM)	SI ^c
29		579 ± 64	356 ± 17	1.6	3030 ± 89	4610 ± 708	8.0
30		76 ± 15	70 ± 14	1.1	2550 ± 77	4710 ± 16	62
31		135 ± 10	113 ± 21	1.2	6690 ± 744	10200 ± 19	76
32		61 ± 9	39 ± 4	1.6	4380 ± 387	6590 ± 845	108
33		31 ± 5	35 ± 5	0.9	2850 ± 66	3540 ± 271	114

^aResistance Index (RI) = *P. falciparum* Dd2 EC₅₀/*P. falciparum* 3D7 EC₅₀.

^bSelectivity Index (SI) = HepG2 EC₅₀/*P. falciparum* Dd2 EC₅₀.

^cSelectivity Index (SI) = MCF7 EC₅₀/*P. falciparum* Dd2 EC₅₀. Antiplasmodial activity determined by SYBR Green I-based proliferation assay in ring stage parasites. Cytotoxicity evaluated by MTS-based viability assay.

Table 5.

In Vitro Metabolic Stability in Mouse Liver Microsomes

compound ID	$T_{1/2}$ (min)	Cl_{int} ($\mu\text{L}/\text{min}/\text{mg}$)
1	79.5	9
6	15.1	46
13	58.1	12
14	50.2	14
15	52.1	13
16	42.5	16
22	65.3	11
30	19.1	36
31	32.4	21
32	40.7	17
33	41.4	17

Author Manuscript

Author Manuscript

Author Manuscript

Author Manuscript

Author Manuscript

Author Manuscript

Author Manuscript

Author Manuscript

Table 6.

Pharmacokinetic Profile of Compound 1

subject	$T_{1/2}$ (h)	T_{max} (h)	C_{max} (ng/mL)	AUC_{last} (min [*] ng/mL)	AUC_{INF_obs} (min [*] ng/mL)	CL_{obs} (mL/min/kg)	V_{ss} (L/kg)	F%
IV(2mg/kg)	4.16	0.08	11,107	411,546	489,317	4.3	0.84	
PO (10mg/kg)	5.71	4.67	153	51,931	98,627	108.9		4.8